राष्ट्र की सेवा में परमाणु
भा प अ कें
BARC
ATOMS IN THE SERVICE OF THE NATION

- Gamma Ray Detector at G20 Summit
- Novel Phoswich Detector
- Dr. Homi N. Sethna Birth Centenary Year

NaI (Tl) CTS
Ref
+-5V

Crystal
TECHNOLOGIES

BARC Newsletter
November-December 2023
ISSN: 0976-2108

INTERNATIONAL YEAR OF
MILLETS
2023

Single Crystal Technology in BARC

Present Status and Way Forward

Single crystals are often required to achieve full functionality of materials exploiting their properties. The design, discovery and growth of novel materials, especially in single crystal form, represent a core competency that is essential for the fulfilment of requirement of advanced scintillator materials and single crystals for radiation detection in power reactors and advanced accelerators. In this regard, the Crystal Technology Section (CTS) of Technical Physics Division (TPD) of Bhabha Atomic Research Centre (BARC) has been at the forefront in the country for several decades.

The CTS of TPD has been involved in the Single crystal growth and characterization of scintillator viz CsI:Tl, NaI:Tl, $Gd_3Ga_3Al_2O_{12}$:Ce, $LaBr_3$:Ce, LiI:Eu, SrI_2:Eu, Lu_2SiO_5:Ce, YAP:Ce, YAG:Ce, pure and doped $Li_2B_4O_7$ by Bridgman or Czochralski crystal growth technique. Further several nuclear radiation detectors and imaging devices which are useful in departmental activities have also been developed by us. These devices have been used for detection of (i) X-ray in the X-ray baggage scanner developed at BARC, (ii) electrons in SEM developed at BARC, (iii) very low dose gamma radiation in waste management plants (WIP and INKARP-BARC), (iv) detection and measurement of X-ray pulse in flash X-ray generators (APPD), and (v) neutron detection (Dhruva Beamline) and beam profile measurement in scynchortron beamlines. The radiation detectors developed by our crystal growth team have been supplied to various laboratories in BARC as well as to other institutions within the country. These developments are in line with the DAE's effort in pursuit of the mission 'Atmanirbhar Bharat' (indigenization). The technology of crystal growth and device fabrication has also been transferred to Indian industries by BARC'S technology transfer unit and the incubation centre to have development of technologically important materials and machines in India.

In an attempt to chalk out the road map for Amrit Kaal period i.e. 2047 for the single crystal growth activity in DAE, a Chintan Baithak was held on 22nd Aug 2023 in BARC. A comprehensive plan to enhance these activities and how to have a complete supply chain of these devices in the country was presented. This thematic BARC Newsletter is yet another step in this direction to bring out the full spectrum of these developments. The Newsletter is quite timely as the use of nuclear radiation involving nuclear detectors as medical diagnostic tools as well as for cancer therapy are in growing demand.

We are grateful to SIRD for giving us this opportunity to bring out this issue compiling the achievements of our team members at CTS, TPD. I am sure that the readers would enjoy the range of articles on crystals and detectors chronicled in this issue.

Dr. S. M. Yusuf
Director
Physics Group
Bhabha Atomic Research Centre

Single Crystals in Advanced and Radiation Technology

We are extremely delighted to get this opportunity to bring out this thematic issue of BARC newsletter on Single Crystals for radiation detection. The Crystal Technology Section of Technical Physics Division is dedicated to the development of scintillator and semiconductor single crystals for the application of radiation detection. This includes crystal growth of conventional scintillators like NaI:Tl and CsI:Tl and advanced fast and high light yield scintillators like $LaBr_3$:Ce and $Gd_3Ga_3Al_2O_{12}$:Ce. These crystals are further processed to fabricate radiation detectors whose performances are comparable to commercially available detectors. Our emphasis is always on having indigenous technologies which are important to the department. Because of the increasing demand for detectors covering a wide range of energy spectrum based on high-purity Ge single crystals in DAE a program was also started for the development of HPGe detectors. We are involved in the growth of Ge single crystals and fabrication of HPGe device by Boron ion implanted and Lithium beam diffusion into High purity Ge single crystals which were commercially bought.

This thematic issue of BARC Newsletter has total five research articles encapsulating the full gamut of the research activities carried out in the Crystal technology Section of Technical Physics division. These articles provide the overview of the different materials we are working on and the detectors developed using them. Further there are two articles detailing recent research highlights of the group and two on the technology transfer, incubation and patent.

We take this opportunity to acknowledge all the authors for their valuable contributions in this thematic issue. We are thankful to Director, Physics Group for his constant support and guidance in compiling the articles. We earnestly acknowledge the guidance of the editors, sincere and hard working role of the editorial team of SIRD for the compilation of the articles, photography of CTS facilities, creative work by the editorial team in designing the cover page and for dedicated efforts in bringing out BARC Newsletter in a time bound manner.

Dr. L. M. Pant
Head, TPD, BARC

Dr. Shashwati Sen
Head, CTS, TPD, BARC

CONTENTS

50

47

BEAM TECHNOLOGY
DEVELOPMENT IN BARC

46

TRON BEAMS & ACCELERAT

This page intentionally left blank

Portable Gamma Detector for G20

①

Single Crystal Growth of NaI:Tl and Fabrication of Gamma Detector for Field Application

G. D. Patra[1]*, S. G. Singh[1], M. Sonawane[1], A. Gupta[2], J. Romal[2], M. K. Sharma[2], Shashwati Sen[1], P. Choudhary[2] and L. M. Pant[1]

[1]Technical Physics Division, Bhabha Atomic Research Centre (BARC), Trombay – 400085, INDIA
[2]Radiation Safety Systems Division, Bhabha Atomic Research Centre (BARC), Trombay – 400085, INDIA

The NaI:Tl detector assembly with the Backpack Gamma Spectrometer System

ABSTRACT

Thallium-doped Sodium Iodide (NaI:Tl), a widely used scintillator material, is commercially available and extensively employed across various departments. In pursuit of detector technology self-reliance, we successfully grew a 2"x2" NaI:Tl single crystal and assembled it with a photomultiplier tube (PMT), compatible preamplifier, and hermetically sealed aluminum housing. Signal processing utilized the indigenously developed Backpack Gamma Spectrometer System (BGSS) at BARC. Rigorous lab and field testing confirmed the detector's characteristics comparable to commercial counterparts, demonstrating its suitability for radiation detection. This DAE in-house made detector was further deployed at the G-20 summit venue for the radiation surveillance.

KEYWORDS: *Gamma Detector, Scintillator, Sodium Iodide (NaI:Tl), Single crystal, Gamma spectroscopy, Photo multiplier tube (PMT), Radiation detector*

Introduction

Scintillators are materials designed to detect high-energy photons and particles, including alpha particles, electrons, and neutrons [1]. They encompass a range of materials such as inorganic and organic crystals, organic liquids, noble gases, and scintillating gases [2]. These materials play a crucial role in converting absorbed energy into visible or ultraviolet photons, enabling detection by photomultipliers and photodiodes [3]. Moreover, scintillators facilitate the accurate measurement of incident radiation's energy and time. Compared to other radiation detectors, they offer enhanced sensitivity to deposited energy, faster response times, and simpler, reliable, and cost-effective construction and operation. Consequently, scintillators find extensive applications in diverse fields such as nuclear plants, medical imaging, manufacturing industries, high-energy particle experiments, and national security [4]. With the years, the demand for scintillators is increasing across the globe. The global scintillator market has witnessed substantial growth in recent years, with its size reaching approximately US\$ 540 million in 2022. According to projections by IMARC Group, the market is anticipated to expand further and reach around US\$ 715 million by 2028. This implies a compound annual growth rate (CAGR) of 4.7% during the period from 2023 to 2028 [5].

NaI:Tl scintillators have a proven track record of reliability and cost-effectiveness, making them indispensable tools in the field of radiation detection and imaging for nuclear physics, medical imaging, and environmental monitoring [6]. Their exceptional performance and broad range of applications have established them as a key choice for commercial customers seeking accurate and efficient solutions for radiation measurement [7]. However, despite its commercial availability,

the Department of Atomic Energy (DAE) in India heavily relies on imports of NaI detectors. To enhance self-reliance in detector technology, a team of researchers from Bhabha Atomic Research Centre (BARC) in Mumbai successfully grew a 2" x 2" single crystal of NaI:Tl and developed a complete detector assembly for radiation detection. This report presents the details of the single crystal growth process, detector fabrication, and the performance evaluation of the indigenously developed gamma detector.

The single crystals of NaI:Tl were grown in a quartz crucible using the Bridgman-Stockbarger technique [8]. The quartz crucibles were thoroughly cleaned and loaded with high-purity NaI and TlI powders. The material was initially dehydrated and sealed. Then the crucible was placed in the Bridgman crystal growth system with controlled heating zones, allowing for the formation of a desired temperature gradient. The temperature of the furnace is increased to melt CsI and after thermalization the crucible is slowly translated to a lower temperature zone for slow and controlled solidification. The grown crystals is taken out of the crucible and were cut, polished, and mounted on photomultiplier tubes (PMTs) using transparent optical cement. The single crystals of NaI:Tl obtained through the growth process were crack-free, transparent, and without inclusions. The crystals were successfully cut and polished into a size of 2" x 2". The mounting of NaI crystals on PMTs was performed with great care to achieve effective optical coupling and prevent air gaps or bubbles. The hermetic sealing of the crystal-PMT assemblies inside aluminum casings provided mechanical support and ensured the integrity of the detectors.

Functional testing of the NaI:Tl detectors was carried out at both laboratory and field conditions. The detectors were connected to the Backpack Gamma Spectrometer System (BGSS), an indigenously developed signal processing system

*Author for Correspondence: G. D. Patra
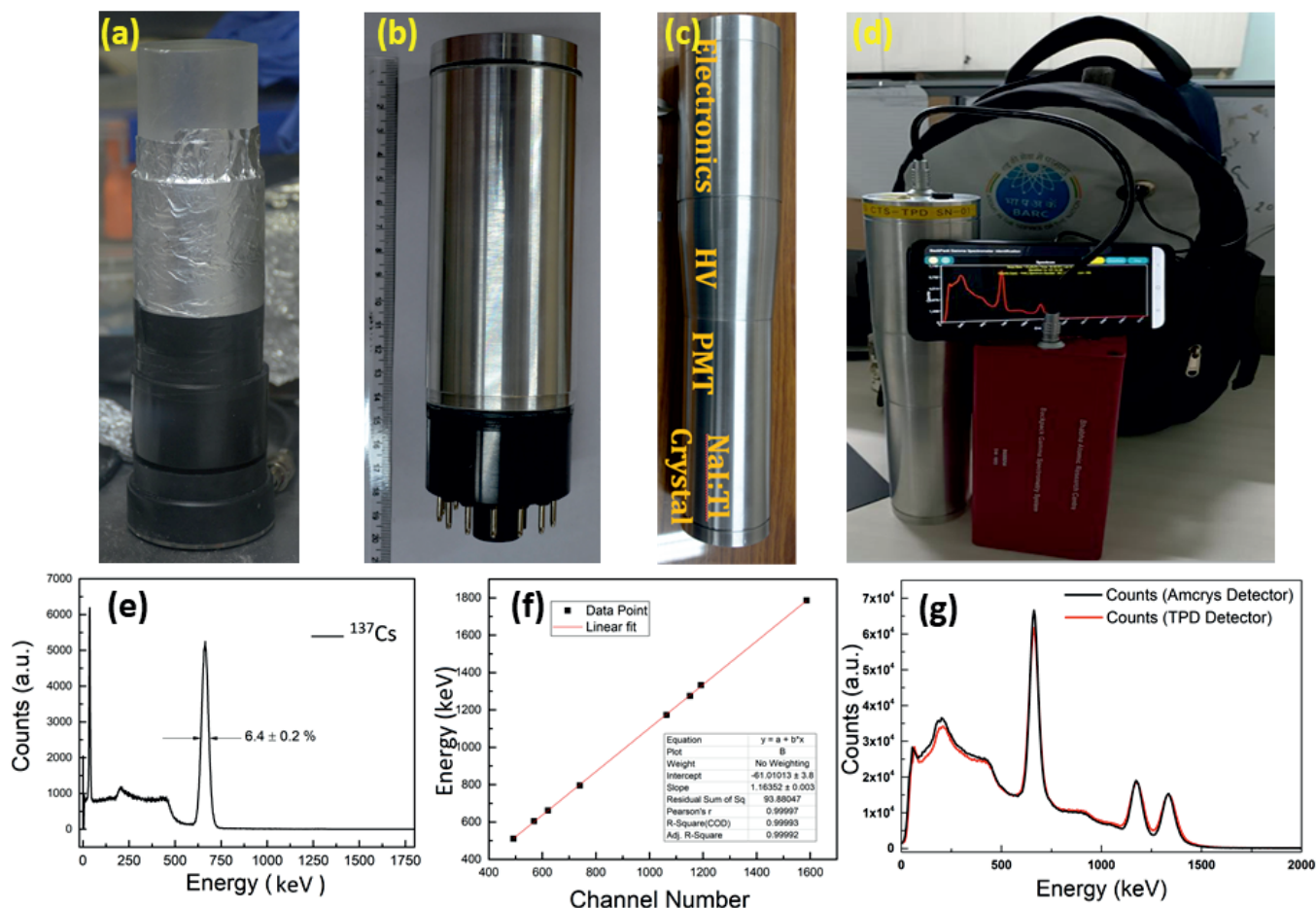E-mail: gdpatra@barc.gov.in

Fig.1: (a) Photograph of the grown crystal mounted on the PMT, (b) Hermetic sealing of the crystal with PMT, (c) the detector assembly, (d) The NaI:Tl detector assembly with the Backpack Gamma Spectrometer System, (e) pulse height spectra for 137Cs source measured using the NaI:Tl based BGSS, (f) Linearity of the detector assembly from 511keV to 1.7 Mev, (g) comparison of the indigenous detector assembly with commercially available Amcrys make detector.

by RSSD, BARC [9]. The detectors exhibited a linear response in the energy range of 500-1800 keV and demonstrated excellent energy resolution. The typical resolution calculated at 662 keV was found to be 6.5 ± 0.2%, comparable to commercial NaI detectors. The stability of the gamma spectrum was evaluated by continuously operating the BGSS system for extended periods, showing no shift in pulse height or change in energy resolution.

The performance of the indigenously developed NaI:Tl detectors was compared with commercially available 2" x 2" size NaI:Tl detectors from Amcrys. The response, resolution, and pulse height of the indigenous detectors were found to be well-matched with the commercial detectors, indicating their comparable performance. 15 such detectors were developed for radiation surveillance at G-20 summit by DAE.

This technological development reduces the department's dependence on imported detectors and also contributes to self-reliance in the Department of Atomic Energy in India as a step towards Atmanirbhar Bharat.

Conclusion

The successful growth of a 2" x 2" NaI:Tl single crystal was achieved indigenously Bridgman-Stockbarger technique to reduce India's reliance on imported radiation detectors. The crack-free crystals were mounted on photomultiplier tubes with hermetic sealing. After connecting to the BGSS, all calibration tests exhibited an excellent energy resolution (6.5 ± 0.2% at 662 keV) and stability. Comparison with commercial counterparts confirmed comparable performance hence leading to the deployment of 15 detectors for G-20 summit radiation surveillance an impactful stride towards Atmanirbhar Bharat in the Department of Atomic Energy.

References

[1]   Knoll, G. F.: Radiation detection and measurement, 3rd edition, John Wiley and Sons, Inc., New York 1999, P. 816.

[2]   Heath, R.L. Hofstadter, R. Hughes, E.B.: Inorganic scintillators: A review of techniques and applications, Nucl. Instrum. Methods Phys. Res. 162(1-3), 431 (1979).

[3]   https://www.hamamatsu.com/content/dam/hamamatsu-photonics/sites/documents/99_SALES_LIBRARY/etd/PMT_handbook_v4E.pdf

[4]   C. Dujardin , E. Auffray, E. Bourret-Courchesne, P. Dorenbos, P. Lecoq , M. Nikl , A. N. Vasil'ev, A. Yoshikawa , and R.-Y. Zhu, Needs, Trends, and Advances in Inorganic Scintillators, IEEE Transactions on Nuclear Science, Vol. 65, No. 8, (2018).

[5]   Scintillator Market: Global Industry Trends, Share, Size, Growth, Opportunity and Forecast 2023-2028, Report ID: SR112023A1378.

[6]   Hofstadter, R.: The Detection of Gamma-Rays with Thallium-Activated Sodium Iodide Crystals, Phys. Rev. 75, 796, Phys. Rev. 75, 1611 (1949).

[7]   K. Akkurt, S. Gunoglu, Arda, S.; Detection Efficiency of NaI(Tl) Detector in 511–1332□keV Energy Range, Sci. Technol. Nucl. Install., vol. 2014, Article ID 186798, 5 pages, https://doi.org/10.1155/2014/186798 (2014)

[8]   Patra, G.D. Singh, S.G. Desai, D.G. Pitale, S. Ghosh, M. Sen, S.: Effect of OH content in the quartz crucible on the growth and quality of CsI single crystals and remedies, J. of Crys. Growth 544, 125710 (2020)

[9]   Gupta, A. Romal, J. Sharma, M.K. Parmar, J.P. Chaudhury, P. Kulkarni, M.S.: (Ed.). Design and development of FPGA based backpack gamma spectrometer. India: Indian Association for Radiation Protection. (2018).

Scintillators

②

Growth of YAP:Ce and its Application for Secondary Electron Detector for BARC-SEM

S. G. Singh[1]*, Siddhartha Shankar Pany[2], G. D. Patra[1], A. K. Singh[1], M. Sonawane[1], Shreyas Pitale[1], Manoranjan Ghosh[1], M. Padmanabhan[2], Shashwati Sen[1] and L. M. Pant[1]

[1]*Technical Physics Division, Bhabha Atomic Research Centre (BARC), Trombay – 400085, INDIA*
[2]*Security Electronics and Cyber Technology Division, Bhabha Atomic Research Centre (BARC), Trombay – 400085, INDIA*

BSE detector developed in BARC

ABSTRACT

Ce doped $YAlO_3$ (Yettrium Aluminium Pervoskite : YAP) scintilllator single crystal of 25 mm dia and 50 mm length has been grown employing Czohralski crystal growth technique. Grown crystal were characterized and processed into detector element for the development of Secondary Electron (SE) and Back-Scattered Electron (BSE) detector for the Scannning electron microscope (SEM) developed at Bhabha Atomic Research Centre. Fabricated SE and BSE detector were tested and qualified for their use in SEM. An ultimate resolution of 20 nm is achieved with SE detectors.

KEYWORDS: *Electron Detector, Secondary electron (SE), Scanning electron microscope (SEM)*

Introduction

Ce doped $YAlO_3$ (YAP:Ce) is one of the excellent scintillators with many advantageous properties like fast decay (~30 ns), good light yield (20-25 k photons/MeV), moderate density (5.3 g/cc) and proportional scintillation response. It is useful in various radiation detection applications like imaging, gamma-ray detectors, timing applications, secondary electron (SE) detector for scanning electron microscope (SEM) and many others [1,2]. Single crystals of YAP are generally grown by the Czochralski technique. The scintillation properties of the materials are highly dependent on the crystal growth parameters [3,4]. In this article we are presenting the growth and scintillation properties of YAP:Ce and development of secondary electron detector.

Growth and Characterization of $YAlO_3$:Ce

Single crystals of YAP:Ce of 60 mm length and 25 mm diameter were grown from the melt using the Czochralski crystal growth technique. Y_2O_3, Al_2O_3 and CeO_2 powders of 99.99% purity were used as starting materials. Powders were mixed in the stoichiometric ratio of 50%Y_2O_3-50% Al_2O_3 (Crystal-I) and 51%Y_2O_3-49%Al_2O_3 (Crystal-II) for the two types of different experiments. The cerium concentration was kept at 0.5 mol% in each experiment. Mixed powders were loaded into an iridium crucible that was placed inside a growth station made from Zirconia based ceramic cylinders. An MF induction heating mechanism based Czochralski crystal puller (Cyberstar, France make Oxypuller) was used to grow the single crystals from the melts. An un-oriented YAP:Ce single crystal of about 6 mm diameter and 40 mm length was used as the seed. A pull rate of about 1 mm/h and a rotation rate of 15 RPM was used in each growth experiment. High pure Ar was used to create inert ambient inside the crystal puller chamber to protect the iridium crucible.

*Author for Correspondence: S. G. Singh
E-mail: sgovind@barc.gov.in

After optimization of growth parameters, large size (25 mm diameter and 50 mm length) high quality transparent single crystals of $YAlO_3$:Ce were grown successfully. A photograph of an as-grown crystal is shown in Fig.1. Grown crystals were free from any visible defects like inclusion, bubbles etc. Single phase formation was confirmed from the powder X-ray diffraction pattern (not shown in the manuscript).

For scintillation characterization 10x10x10 mm^3 samples were cut from the crystal ingots as shown in Fig.2. Radio-luminescence of the samples was recorded using a white X-ray source (Cu-target) operating at 40 kV - 30 mA and a mono-chromator. All the experiments were carried in 45 degree reflection geometry. The recorded photoluminescence spectra are shown in Fig.3 and are not corrected for the instrument response. It shows the characteristic spin allowed transition of Ce^{3+} centre in YAP. The luminescence spectra exhibited the characteristic Ce^{3+} emission (370 nm) corresponding to 5d→4f transition [2]. The radio-luminescence spectra for both types of
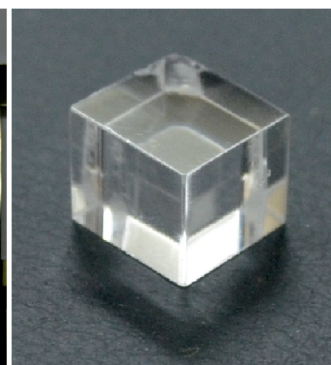

Fig.1: Single crystal ingot of YAP:Ce.

Fig.2: Single crystal sample cut from ingot and processed for characterization.
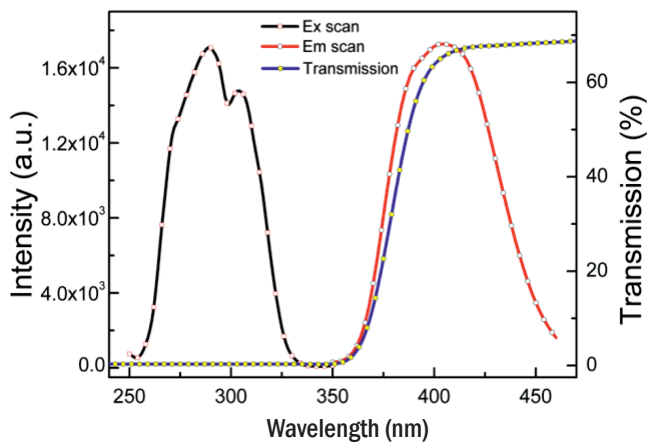
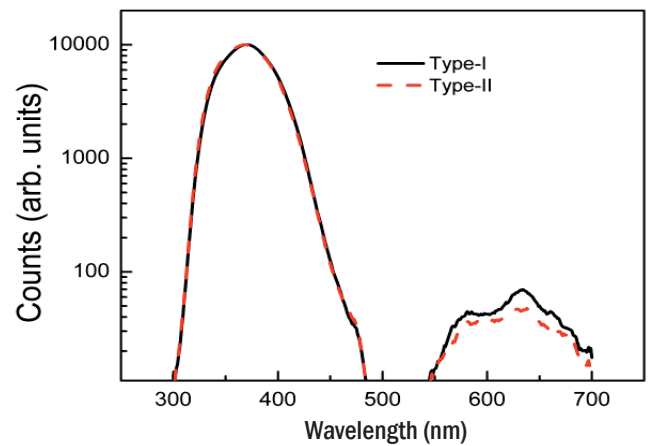Fig.3: *Photo-luminescence and transmission spectra of YAP single crystals.*

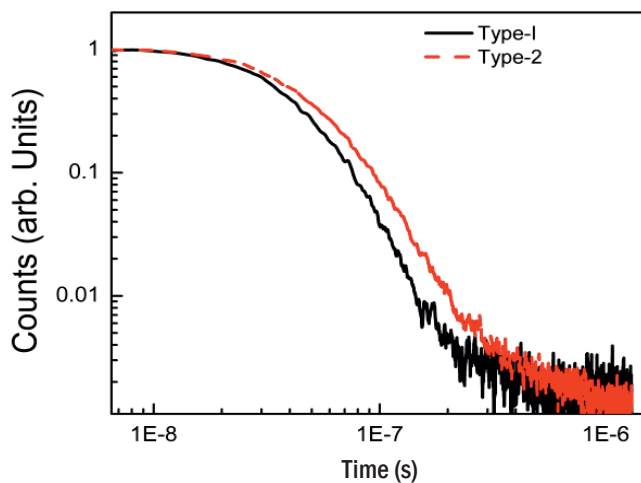Fig.4: *Radio-luminescence spectra of YAP single crystals.*

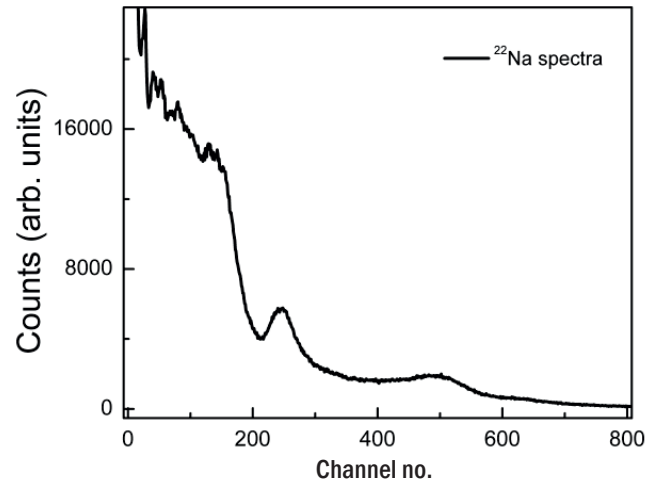Fig.5: *Decay profile of type-I and type-II crystals (for gamma excitation).*

Fig.6: *Pulse height spectra of ^{22}Na recorded using a 10x10x10 mm^3 YAP:Ce.*

crystals are shown in Fig.4. In RL, an emission at longer wavelength (600 nm) accompanied the Ce characteristic emission in both types of crystals. Though the 370 nm emission remains insensitive to the stoichiometric variation in the melt, the contribution of longer wavelength emission is relatively less in type-II crystals. That may be because of less number of Y^{3+} related defects in the type-II crystals.

For pulse height and decay time measurements, one face of the cube was polished to optical finish and on remaining faces 5-6 layers of Teflon tape were wrapped. The polished face was then coupled to a PMT (R6095) using silicone based optical grease. An AMPTEK-DP5G MCA was used to record the pulse height spectra (^{22}Na source) while a TEKTRONIX (MDO3102) digital storage oscilloscope was used to record decay profile. The recorded decay profiles (for gamma excitation) of the type-I and type-II crystals are shown in Fig.5. It may be seen that the decay profile of type-I crystal is faster (~30 ns) than that of type-II crystal (~38 ns). This difference in the decay profile may be explained on the basis of different kinds of traps in the two types of crystals which are also observed in the RL spectra. The pulse height spectra (Fig.6) of both types of crystals were almost identical and is comparable with reported spectrum for YAP:Ce [1]. The energy resolution measured for the ^{22}Na gamma source was ~7% at 511 keV. From these results it is concluded that the stoichiometric variations in the melt considerably affect the timing and other scintillation properties of Ce doped YAP crystal scintillator and crystals grown from stoichiometric ratio of $Al_2O_3:Y_2O_3$ yields

better result. For further application only crystals grown from stoichiometric charge (type I) were considered.

Development of Detectors for Indigenous SEM

SE detector

Secondary Electron (SE) detector is a fundamental part to any general-purpose SEM, as it facilitates imaging of the specimen's topographic features. Secondary electrons (SE) (~1-50eV with mean energy ~5eV) are generated through primary electron beam interaction with specimen. The detection of SE involves acceleration of the SE's to a voltage around 10 keV and using scintillators as detecting element for these accelerated electrons.

The SE detector for BARC-SEM has been designed on this principle that is primarily based on Everheart-Thonley (ET) detector (Fig.7). The detector comprises of 10 mm diameter, 1 mm thick YAP:Ce scintillator single crystal maintained at a voltage of +10 kV to accelerate the secondary electrons. The scintillator is interfaced with fused silica light-guide which is connected to a PMT on the other end. The attractor electrode is maintained at a voltage ranging between +1 kV to -1 kV. While the purpose of the attractor electrode for most SE detectors is to attract the low energy SE towards the detector, the purpose of this electrode in the current design is to focus the stray SE towards the scintillator. In this detector configuration, the electric field generated by scintillator potential directly exerts attracting force on SE.
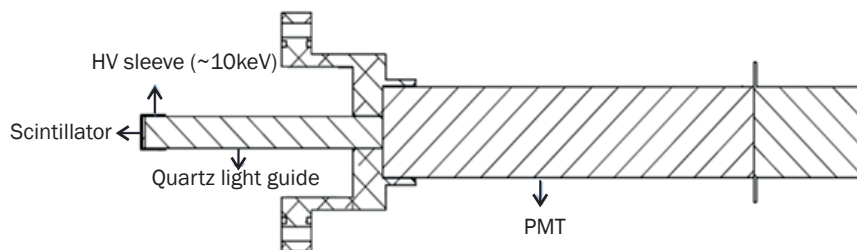
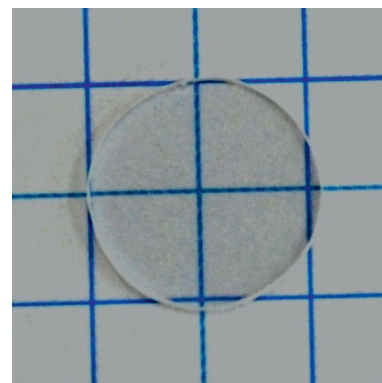Fig.7: Schematic of ET design based SE detector for BARC-SEM.

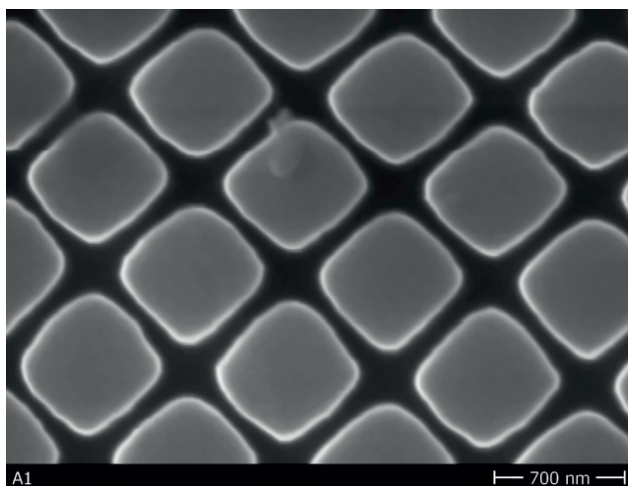Fig.8: Processed YAP:Ce scintillator (10 mm dia, 1 mm thickness).

Fig.9: Magnification:1,00,000x, Specimen: SEM Calibration Sample (Recorded employing developed SE detector).
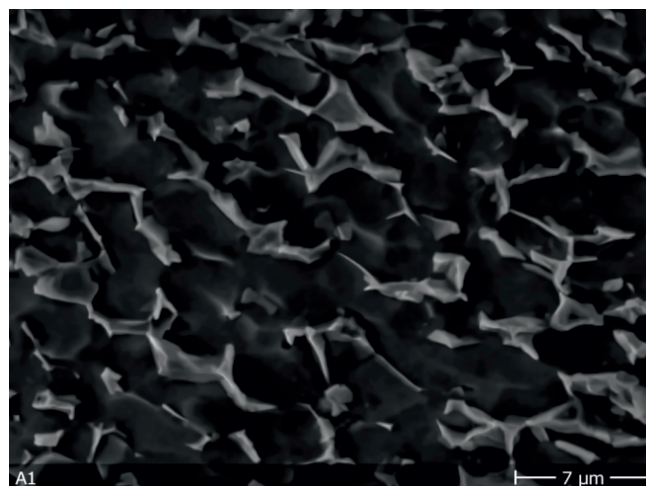

Fig.10: Magnification:10,000x, Specimen: Zr - 2.5% Nb (Recorded employing developed SE detector).

The choice of YAP:Ce as scintillator for SEM detectors is based on its resilience to electron-beam impact, fast decay constant of ~ 30 ns, low after-glow and relatively good photon yield. Single-crystal YAP:Ce scintillators for the detectors have been grown in house using Czochralski crystal growth technique as discussed in the above section. The crystal in the form of ingot of dia. 25 mm and 50 mm length has been processed into scintillators of suitable diameters and 1mm thickness Fig.8. The scintillator disc was polished to optical finish. To prevent electron impact induced charge accumulation on scintillators a 50 nm thick Aluminium layer is deposited on the scintillator crystal outer surfaces using thermal evaporation system. The aluminium layer also functions as a specular reflector for back-propagating scintillation light-rays, and thus enhancing the light collection at PMT. The detector was tested for its performance by incorporating it in a SEM machine and typical images at higher magnification are shown in Fig.9 and 10.

BSE detector

The BSE detector is an annular thin plate detector that is placed near the bottom plane of the objective lens. The incident electrons pass through the centre hole of the detector and fall on the sample. Interaction of electron beam with a sample target produces a variety of elastic and inelastic collisions between electrons and atoms within the sample. Elastic scattering depends on atomic number of atoms, consequently, the number of backscattered electrons (BSE) reaching a BSE detector is proportional to the mean atomic number of the sample. Thus, BSE images are very helpful for

obtaining high-resolution compositional maps of a sample and for quickly distinguishing different phases. The BSE detector is similar to the E-T detector. These consist of an Al coated scintillator coupled to a photomultiplier by a light guide. Scintillator based BSE detector can be used down to primary beam energy upto 1.5 keV.

BSE detector designed for BARC-SEM consists of an annular scintillator YAP:Ce crystal of OD 25 mm, ID 6 mm and thickness 1mm. The scintillator is mounted onto a specially designed quartz light-guide, which interfaces with a PMT on the other end (Fig.11). The BSE detector has been designed to double-up as SE detector also, upon application of a positive potential of +10 kV to the scintillator. For fabrication of the detector a disc of 25 mm dia and 2 mm thickness was cut from crystal ingot and processed in to optical finish. An annular hole was cut at the center of the scintillator disc for primary electron beam to pass. The whole assembly was tested for its performance by recording the BSE image shown in Fig.12.

Conclusion

The process for growth of YAP:Ce single crystal is developed. The grown crystals were characterized for their performance and were suitable for scintillator applications like x-ray detection and application in SE detectors etc. The crystal was further processed for development of SE detector for BARC-SEM being developed at SESSD. The full process starting from crystal cutting, lapping and polishing to design and fabrication of whole detector assembly was carried and performance of the detector tested in SEM that achieved an ultimate resolution of 20 nm.
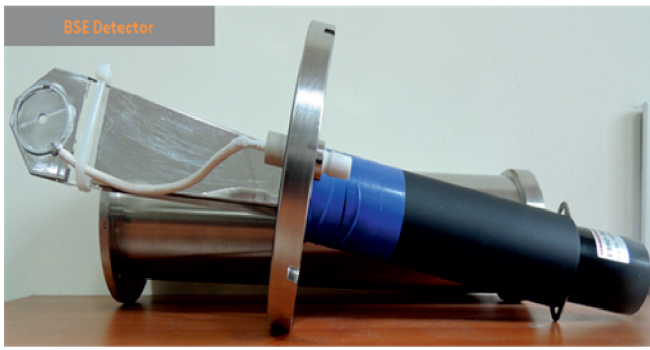
Fig.11: Developed BSE detector.
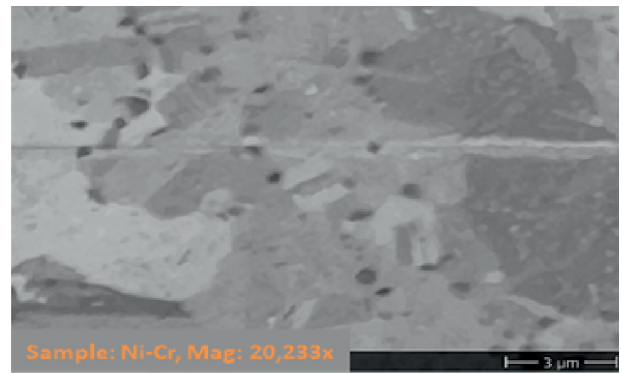
Fig.12: BSE Image of sample Ni-Cr alloy at mag: 22,000.

References

[1]   Alshourbagy, et al. J. Crystal Growth 303 (2007) 500–505.

[2]   R. Pani, F. de Notaristefani, K. Blazek, P. Maly, R. Pellegrini, A. Pergola, A. Soluri, F. Scopinaro, Nucl. Instr. and Meth. A, 348 (1994) 551.

[3]   B.G. Baryshevsky, et al. J. Phys.: Condens. Matter 5 (1993) 7893-7902.

[4]   M. Moszyński, M. Kapusta, D. Wolski, W. Klamra, B. Cederwall, Nucl. Instr. and Meth. A, 404 (1998) 157.

Gamma Imaging

③

Development of 2D Scintillator Array from CsI:Tl Single Crystal for Gamma Imaging

S. G. Singh[2,3]*, **Murali Ravi**[1], **Koushik V.**[1], **D. S. Sisodiya**[2,3], **G. D. Patra**[2], **Sumukh Nandan**[1], **Shashwati Sen**[2,3] and **S. S. Sai**[1]

[1]Department of Physics, Sri Sathya Sai Institute of Higher Learning, Puttaparti, Andhra Pradesh – 515134, INDIA
[2]Technical Physics Division, Bhabha Atomic Research Centre (BARC), Trombay – 400085, INDIA
[2]Tata Institute of Fundamental Research, Mumbai – 400085, INDIA
[3]Homi Bhabha National Institute, Mumbai – 400094, INDIA
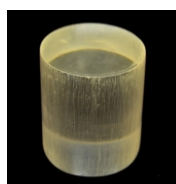
Processed CsI:Tl single crystal of diameter 50 mm and length 50 mm under UV illumination

ABSTRACT

A Gamma camera was developed using a 2 dimensional array of 8 x 8 CsI:Tl single crystals grown at BARC. The scintillator array was mounted on position sensitive PMT (PSPMT) to fabricate the detector. Acquisition and image process algorithm were implemented to achieve a spatial resolution of 5 mm. The device has been integrated to be used as a intra-operative tool to detect tumors using radioactive tracers.

KEYWORDS: *Scintillator array, Crystal, Gamma*

Introduction

CsI:Tl scintillator has been extensively used for X-ray and Gamma-ray imaging which are required in various applications like industrial inspections nuclear medicine imaging, and scientific research [1,2]. In these applications the scintillator is coupled to position sensitive photo-multiplier tube (PSPMT), photo-diodes or Pixelated Si-PM is used. For imaging of a radioactive source with directional information there are various schemes like coded-aperture imaging, Compton imaging, and Directional-Sensitive Array detector. The spatial resolution of the system is governed by the size of the scintillator pixel as well as the electronics.

In this paper, we are reporting on the growth of CsI:Tl single crystal and a cost-effective process for fabrication of scintillation detector array from the single crystal which realizes a spatial resolution of around 5 mm as well as a spectral resolutions (~15% FWHM). We have developed a process where pixels are fabricated with very high precision from the in-house grown CsI:Tl single crystals. The developed 2D scintillator system consisting of a 8 × 8 CsI (Tl) array coupled with a 8 × 8 array of PSPMT and a compact readout along with image processing algorithm is developed.

Experimental

Single crystals of CsI (Tl) of 50 mm diameter and 75 mm length were grown by the vertical Bridgman technique using a furnace having four separately controlled zones. These Bridgman furnaces for the growth of halide single crystals have been designed in-house and fabricated locally. Fig.1 shows various Bridgman furnaces located at CTS, TPD.

For the single crystal growth, all materials used were of 99.999% purity. Tl is used as the dopant in the CsI matrix. The powder material were initially taken in a quartz ampoule (Fig.1(b)) and sealed after dehydrating so as to remove any moisture content from the powder sample. After sealing the quartz crucible was loaded in the Bridgman furnace and heated so as to melt the loaded power. After that the crucible is translated from the hot zone of the furnace to the cold zone at a rate of ~1mm/hr to solidify the melt into a single crystal. After the completion of the growth the quartz is cut and the crystal is retrieved (Fig.2(a)). The grown crystal was characterized for its scintillation characteristics and an energy resolution of <7% at 662 keV was recorded as shown in Fig.2(b).

For fabricating the 2D array of the CsI scintillator, the grown crystal were processed in to the pixels as per the schematic shown in Fig.3. In the first step the cylindrical crystal was shaped into a cube and eight plates of size 50 mm x 40 mm x 5.7 mm were cut using a diamond coated copper wheel. These plates were stacked together and glued to each other

Fig.1:(a) Bridgman furnaces with an operating temperature of 1000⁰C maximum, located at CTS, TPD used for the growth of halide scintillator single crystals. (b) Quartz crucible used for the growth of CsI single crystal.

*Author for Correspondence: S. G. Singh
E-mail: sgovind@barc.gov.in
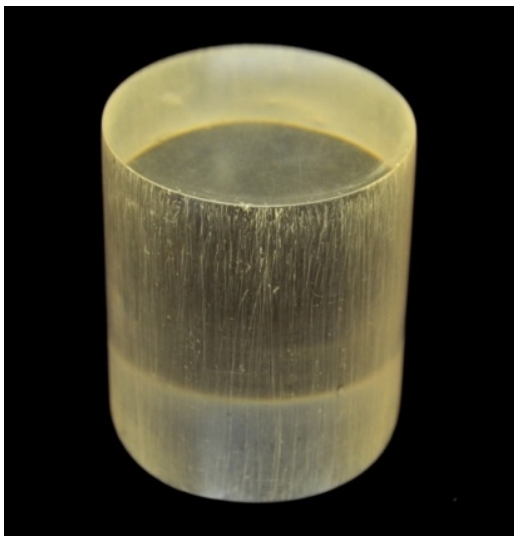
Fig.2: (a) Photograph of a processed CsI:Tl single crystal of diameter 50 mm and length 50 mm under UV illumination.
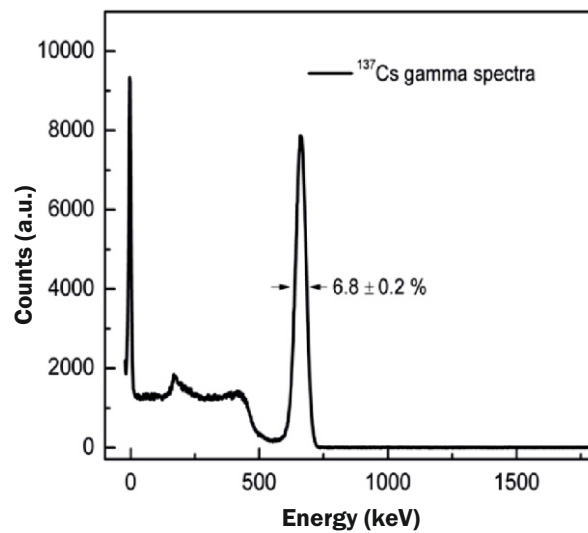
Fig.2: (b)The Pulse height spectra of ^{137}Cs source measured using the grown CsI single crystal.

using optical cement mixed with TiO_2. TiO_2 is used as a reflectent coating which inhibits crosstalk among the pixels. The process of cutting and stacking is repeated so as to get a plate consisting of 8 x 8 matrix of CsI crystal pixels each of size 5 mm x 5 mm x 5 mm.

Results and Discussion

A 8 x 8 pixel array of CsI:Tl is developed with individual pixel size of $5 \times 5 \times 5$ mm^3 with a separation of 0.3 mm to match the pitch of the PSPMT. However the process is suitable to make smaller pixels down to the size of 1 mm and separation of 0.1 mm. To achieve the separation between two pixels a reflective layer based on TiO_2 and Epoxy was developed to get optical isolation as well as good adhesion to keep pixels together. Loading of TiO_2 was optimized to 70 wt% of epoxy to get best results in terms of reflectivity and mechanical stability. Fig.4 shows the photograph of the stacked crystals, the 2D matrix of the crystals and the 2D matrix mounted on the PSPMT forming the full device.

We developed an algorithm that facilitates interaction with the detector, enabling real-time streaming and extended single-frame data acquisition capabilities as shown in Fig.5. The acquisition and imaging processes are designed as a two-threaded system, as illustrated in Fig.6. This can be broken down into key elements as follows:

- **Buffer Initialization and Network Configuration:** A data buffer is initialized, and network settings are configured using Winsock libraries.

- **Data Reception and Buffer Management:** This function continuously receives data and employs circular buffer management to prevent overflow.

- **Data Processing and File Handling:** This function processes and writes data to CSV files, efficiently managing up to 1000 files to avoid overwriting.

- **Multi-Threading for Continuity:** Two threads for uninterrupted data reception and file management runs concurrently.

- **Main Function and Thread Handling:** The main function directs the entire process, creating threads for data flow and processing, and subsequently closing thread handles upon completion.

In the optimized acquisition algorithm, we have mitigated the inherent latency in reading and displaying the output by integrating the imaging algorithm into the acquisition thread
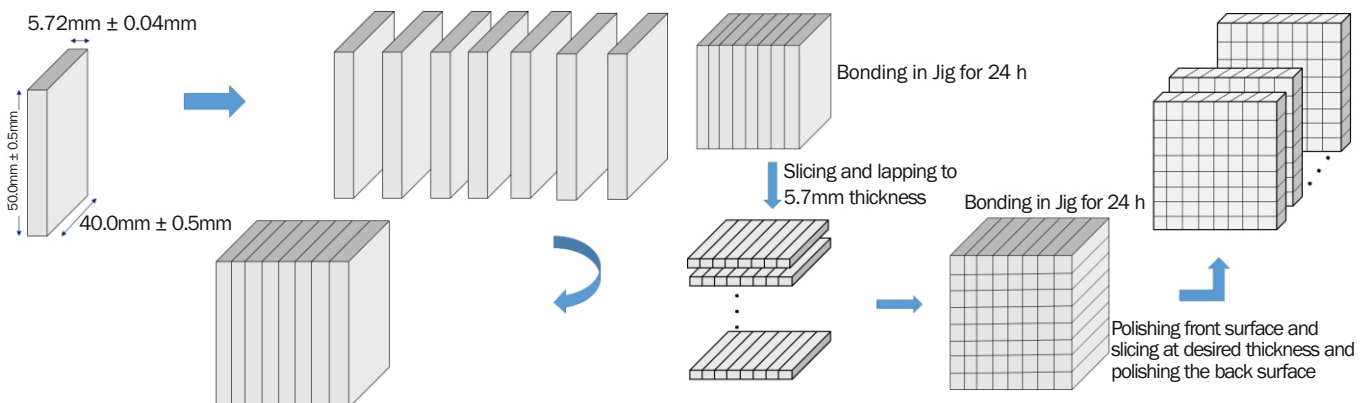
Fig.3: Schematic of process for pixel array fabrication.
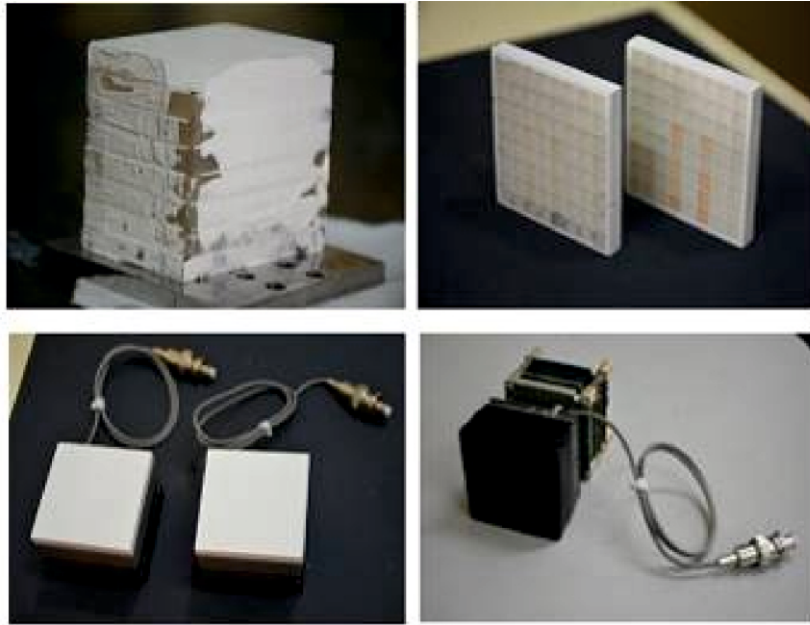
Fig.4: 2D- array of CsI:Tl (8x8) mounted on PMT.
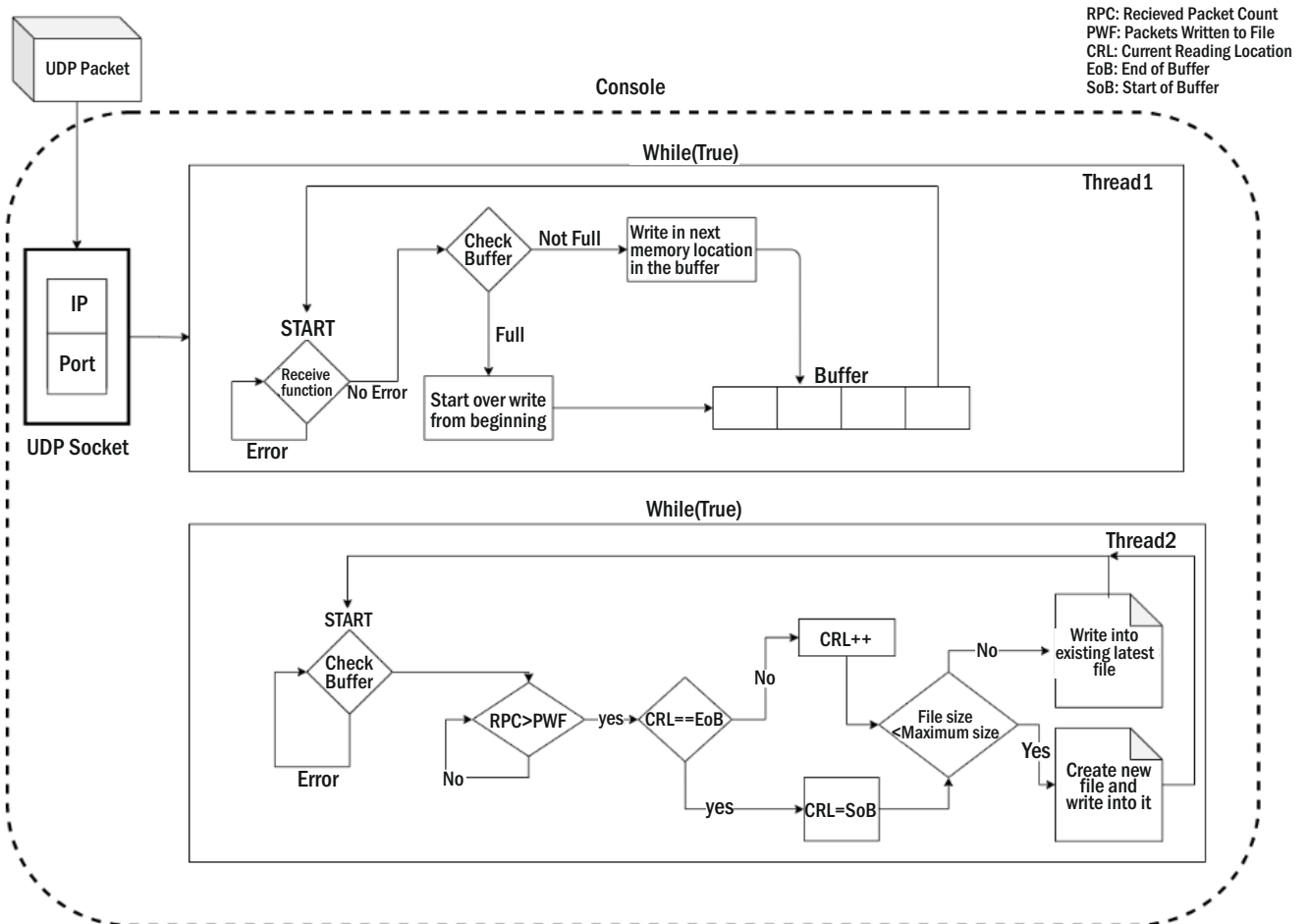
Fig.5: Acquisition Algorithm.

itself. This optimization enables the simultaneous retrieval of both the display and the log file, without dependency on log file creation. As a result, this enhancement has significantly reduced time complexity compared to the unoptimized code. In the trigger-time mode, acquired scintillations are binned into an 8 x 8 format, yielding an average frame rate of 50 frames per second. The algorithm is deployed using the C++ programming language and the detector's performance is assessed using two types of lead slits (horizontal and slant) with an ^{152}Eu 0.5 mCi source kept at 4 inches from the detector.
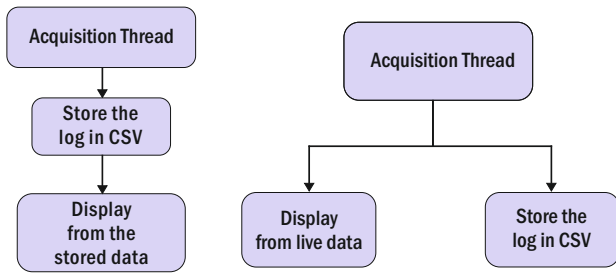
Fig.6: Unoptimized Acquisition (left) ; Optimized Acquisition (right) .
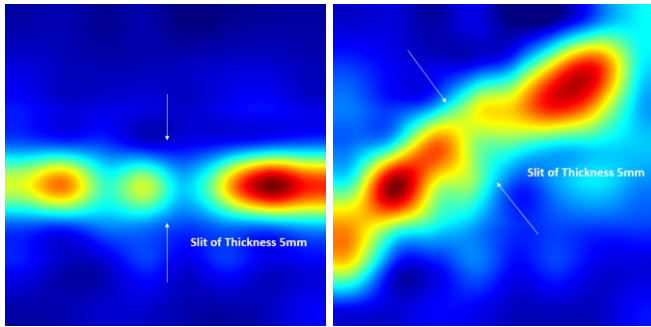
Fig.7: Real-time imaging with optimized code with two slits (left) horizontal and (right) slant.

Fig.8: Cotton phantom containing radionuclide (Top); Image of the cotton phantom detected using Gamma Camera (Bottom).

Incorporating the scintillator detector and the slits, a hand held gamma camera was developed. The working of this device was tested in the lab using a cotton ball dipped in liquid radionuclide and the real time image was recorded as seen in Fig.8. Further testing of the device will be carried out in hospital for detection of cancerous tissues in the operation theater.

Conclusion

A gamma camera using a 8 x 8 matrix of CsI:Tl single crystals of dimension 5 x 5 x 5 mm each was developed. The scintillator matrix was coupled with a PSPMT and algorithm was developed to enable real-time streaming of data and image processing. The development is aimed to fabricate a gamma camera which can be used as an intra-operative tool for imaging of cancerous tissues using radioactive tracers.

References

[1] Qianru Zhao et al, Nucl. Inst. Phys. Res. A, 1040 (2022) 166985.

[2] J.R. Deepak et al, Mater. Today Proc. 44 (2021) 3732–3737.

Solid-state Detectors

4

Development Journey of Eu^{2+} doped LiI Single Crystal Based Portable Solid-state Detectors for Thermal Neutrons

Awadh Singh*, M. Tyagi, S. G. Singh, G. D. Patra, D. S. Sisodiya, Sonu and Shashwati Sen

Technical Physics Division, Bhabha Atomic Research Centre (BARC), Trombay – 400085, INDIA

A hermetic sealed LiI:Eu detector

ABSTRACT

Single crystals of Eu-doped LiI are well known for their potential applications to be used as a scintillator to detect thermal neutrons. However, the growth of these single crystals are challenging due to their hygroscopic nature, sticking to the crucible and inclusions. We have successfully addressed all these problems for the growth of single crystals of LiI: Eu. Detectors fabricated from these in-house grown crystals were used in the Pulse height measurements for thermal neutrons.

KEYWORDS: *Crystal growth, Scintillator, Neutron Detector, Thermal Neutrons*

Introduction

Neutron detectors serve a wide range of applications, spanning research, defense, security, and nuclear industries. Conventional neutron detectors utilizing gas-based systems, predominantly rely on ^{3}He and BF_3 gases, exhibit suboptimal efficiency levels. Poor gamma discrimination, wall effect are some of the challenges which limits the applications of the gas based thermal neutron detectors in the field applications [1,2]. In contrast, europium- activated lithium iodide emerges as a well- established scintillator with particular utility in thermal neutron detection. The deployment of europium-doped lithium iodide in single crystal form bestows substantial advantages, including higher detection efficiency, as well as enhanced portability and compactness compared to gas-based detectors. Moreover, its capability to detect both gamma rays and thermal neutrons extends its application scope. In europium-doped lithium iodide (LiI: Eu), the naturally occurring isotope ^6_3Li is endowed with a significant absorption cross-section(~940 barns) for thermal neutrons. Consequently, this is instrumental in a 'Q' value energy of 4.8 MeV effectively getting deposited within the scintillator [1]. This inherent characteristic facilitates robust pulse height differentiation between low-energy gamma radiation and thermal neutrons. Upon the engagement of thermal neutron with ^{6}Li leading to (n, α) ^3_1H reactions, the produced charged particles excite the Eu^{2+} ions, inducing a scintillating emission lasting a few microseconds within the blue region (~470 nm) of the electromagnetic spectrum. This emission profile harmonizes seamlessly with the responsiveness of Bialkali photomultiplier tubes(PMTs), thus rendering standard pulse processing electronics comprising pre amplifiers, shaping amplifiers, and Multi-channel analyzers (MCA) for the readout purposes [1,3].

However, it's essential to acknowledge that the hygroscopic tendencies of lithium iodide impart a significant dependence of the crystal's scintillation property on growth processes. Consequently, a challenge arises in maintaining consistent scintillation responses across single crystals originating from the same charge, unless the entirety of the growth procedure is meticulously optimized. To address this, the present paper delves into a comprehensive discourse on the recipe of the single crystal growth procedure and the detector fabrication for the thermal neutron detectors employing lithium iodide single crystals at its heart.

Experimental

Single crystals of Lithium Iodide doped with 0.1% Europium (LiI:Eu) were successfully grown utilizing the Bridgman technique. The growth procedure involved using high- purity, anhydrous LiI and EuI$_2$, enclosed within a quartz ampoule under an argon atmosphere. Specially designed quartz crucibles are prepared through etching with a 10% HF solution for 5-7 minutes, followed by baking at 700 degrees Celsius for 10 hours under rotary vacuum conditions. The prepared crucible was transferred into a glove box through a right-angle valve under vacuum conditions, assuring an oxygen and moisture content of less than 0.1 ppm. The initial charge comprised ultra-dry anhydrous beads of LiI (^{6}Li with a natural abundance of 7.4%) and EuI$_2$, both possessing a purity of 99.99%. These components were combined in a stoichiometric ratio to have a 0.2 mole% doping of Eu in the LiI matrix. Subsequently, the mixture was subjected to dehydration within the quartz ampoule at 300^{0}C for a span of 4 hours under a running vacuum of 5 x 10^{-5} mbar to eliminate any residual moisture or oxygen. The sealing of the quartz ampoule was ultimately executed under a continuous vacuum. This sealed ampoule was then positioned within a Bridgman furnace, wherein it was heated to 510^{0}C and maintained at this temperature for 4 hours to achieve thermal equilibrium in the melt. The process of single crystal growth initiated as the ampoule was gradually lowered through a temperature gradient of approximately 12-15 K/cm. This lowering procedure consisted of an initial phase at a rate of 0.2 mm/h within the cone region, followed by a rate of 0.5 mm/h in the

*Author for Correspondence: Awadh Singh
E-mail: awadhks@barc.gov.in
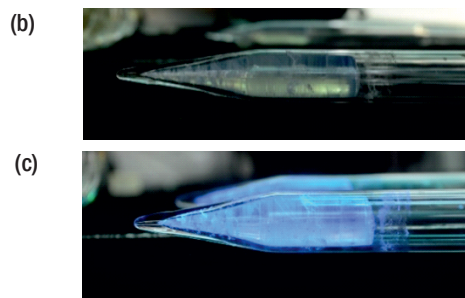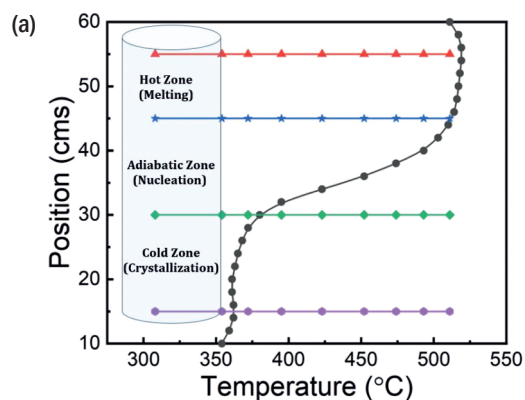
Fig.1: A typical Bridgman Crystal Growth Furnace.

Fig.2 (a):Temperature gradient profile used for the growth of $LiI:Eu^{2+}$.
(b) As grown single crystal inside quartz ampoule.
(c) As grown single crystal inside quartz ampoule under UV radiation.

cylindrical region. Upon the completion of crystal growth, the quartz ampoule housing the grown single crystal subjected to a 10-hour annealing at $450^{o}C$. This annealing step aimed to mitigate thermal stresses in the crystal arising from contact between quartz and crystal. Subsequently, the grown crystals were gradually cooled down to room temperature at a controlled rate of $10-15^{o}C$ per hour. To retrieve the grown single crystals, the quartz crucible was dissected under the protection of silicon oil. This approach was taken to prevent any potential contact with moisture or oxygen, which could compromise the single crystal's properties. The structural characteristics of the grown crystals were studied using Powder XRD and the powder samples were wrapped in a kapton sheet to protect the samples from oxygen and moisture during the data collection. The samples were found to be chemically stable during and even after the measurements for few hours. For the optical and scintillation measurements, the samples were prepared from the as-grown single crystals within the glove box. The Radio-luminescence (RL) properties were evaluated using a monochromator with compatible software (Princeton Instruments Acton spectrapro SP-2300). For excitation, a white X-ray source with a Cu target, operating at an accelerating voltage of 40 kV and a tube current of 30 mA, was employed. Scintillation measurements were performed on a processed scintillator measuring 10 mm, 25 mm and 50 mm in diameter and 2 mm approx. in thickness. This scintillator was hermetically sealed within a cylindrical aluminum container, with a high-purity quartz plate on one end. A diffused reflector (Al_2O_3) was incorporated in the aluminum container to facilitate efficient light collection from the quartz plate. Ultimately, a Hamamatsu PMT was coupled to the LiI: Eu scintillator for thermal neutron measurements.

Results and Discussion

Fig.1 shows the photograph of the Bridgman furnace designed by CTS, TPD and fabricated with the help of the local industry for the single crystal growth of low temperature halide single crystals. The gradient of the furnace with two isothermal zones operating at the melting temperatures and separated by an adiabatic zone created by the baffle has been shown Fig.2. 4N pure LiI and EuI_2 (Source: Lanhit) were used for carrying out the single crystal growth experiments. A freshly grown single crystal of Lithium Iodide doped with 0.1% molar concentration of Europium grown using the Bridgman furnace developed at CTS, TPD is shown in Fig.2b. The single ingot exhibits a pristine, crack-free structure without any observable defects and crack-free structure. The same crystal under UV light is shown in Fig.2c. and shows strong luminescence in the blue region.

The single crystals were grown with a lowering rate of 0.1 mm/hr in the nucleation region and the lowering rate was varied in the range of 0.2 mm to 0.5 mm per hour in the cylindrical region. It has been found that if the material dehydration is good which is observed directly from the vacuum during dehydration a higher pull rate up to 0.5 mm/hr for crystal up to 1-inch diameter can be employed. However, the dehydration for less than 4 hours and temperatures below $300^{o}C$ leads to inclusions in the grown crystal along the length which segregate at the end of the cylindrical region. It has also been found beneficial to dehydrate the material before the doping up to 6 hours and then dehydrate again for 2 hours after Eu^{2+} doping. However, this dehydration process is also affected by the amount of starting charge and multiple dehydration cycles were found to be beneficial if the starting charge is more than 100 g. Usually, 350 g of starting charge were loaded in a 2-inch quartz ampoule for the growth of a 2 inch diameter and 2-inch length single crystal, and required much longer dehydration time to achieve transparent single crystals. Post growth, the retrieval of the single crystal was easy in 15 mm diameter single crystals. However, the crystal growth experiments carried out for 1-inch and 2-inch diameter single crystals results in sticking to the crucible wall and cracking during or after the growth. We could address the sticking problem for the 1-inch single crystal by optimizing the
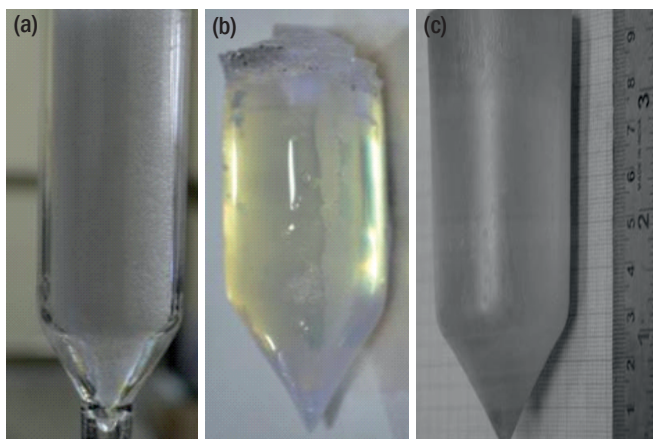
Fig.3: (a) A Quartz ampoule loaded with starting charge of LiI: Eu^{2+}.
(b) A 1-inch diameter single crystal of LiI: Eu^{2+}.
(c) A 2-inch diameter single crystal of LiI: Eu^{2+}.

Fig.4: Powder XRD Pattern of LiI:Eu^{2+}.

dehydration time but for the 2-inch single crystals the sticking to the walls couldn't be restricted. Hence, we employed inversion technique where the whole furnace was inverted after the completion of the growth experiments and temperature were raised for the region where grown single crystal lies to melt the crystal from the surface and glide it to the region where the temperature was reduced just below melting point. The thermal shock was minimized in this process and damping mechanism were used to minimize the mechanical shock during the glide of the grown single crystal inside the crucible. We could successfully address this issue also by carrying out the crystal growth experiment in carbon coated quartz ampules and transparent and crack free single crystals were achieved for both 1-inch and 2-inch diameter. The Photographs in Fig.3a. shows the quartz ampoule loaded with LiI: Eu^{2+} while the Fig.3b and 3c. shows the as grown single crystal ingot for the 1-inch and the 2-inch diameter single crystals. We have observed core formation in the 2-inch diameter single crystal when the lowering rate was higher than 0.2-0.3 mm per hour and we couldn't completely address this issue. The non-uniform segregation of Eu^{2+} in LiI matrix along with the initial purity of the starting charge are a few possible reasons and we are addressing this issue by purifying the starting charge with multiple crystallizations.

The grown crystals were also characterized for their structural properties and the power XRD measurent were carried out in the range of 10-80° and the XRD pattern is shown in Fig.4. It confirms the phase of the grown crystal without any additional peaks which may have arisen due to oxygen or moisture contamination as the material is quite reactive to the moisture/oxygen at elevated temperatures. We have observed two additional peaks arising from the polythene sheets used to wrap the powder to protect it and have been marked as SH. Optical characterization was carried out on the transparent and core free region of the grown single crystals. The UV response of the same crystal is shown in Fig.5. It shows transmission of around 45% in the 450-500 nm range with ~20% reflective losses at windows surface of the sample holder. A cut off at 450 nm have been found in the transmission due to the absorption of light in the Eu^{2+} energy levels [3,4]. The radioluminescence spectrum shown in Fig.6. features a prominent emission band peaking at approximately 470 nm, accompanied by a minor tail at the higher wavelength range. This emission band aligns with electron transitions within the Eu^{2+} ions (5d → 4f) embedded in the LiI matrix. However, no discernible signatures of Eu^{3+} bands were detected [3, 5]. The comparison of transmission and radioluminescence suggests significant self-absorption in large crystal dimensions due to

Fig.5: Transmission Spectrum of LiI:Eu^{2+}.
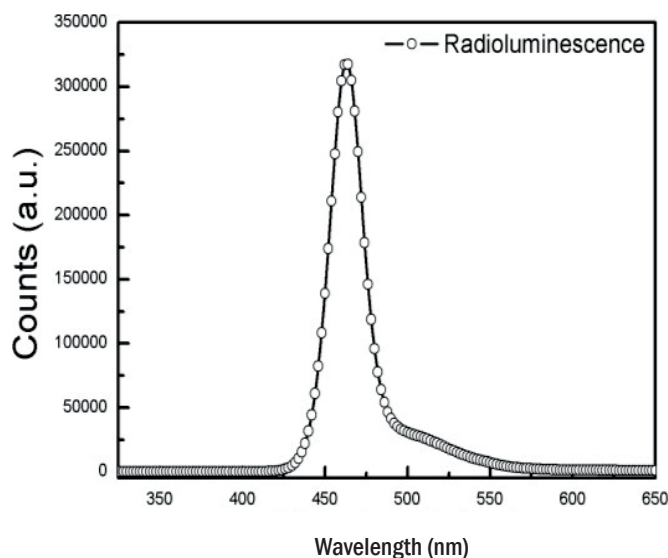
Fig.6: X-ray induced Luminescence from LiI:Eu^{2+}.

Fig.7: A hermetic sealed LiI:Eu detector.

Fig.9: Pulse height spectrum due to thermal neutrons with standard flux from LiI:Eu^{2+}.
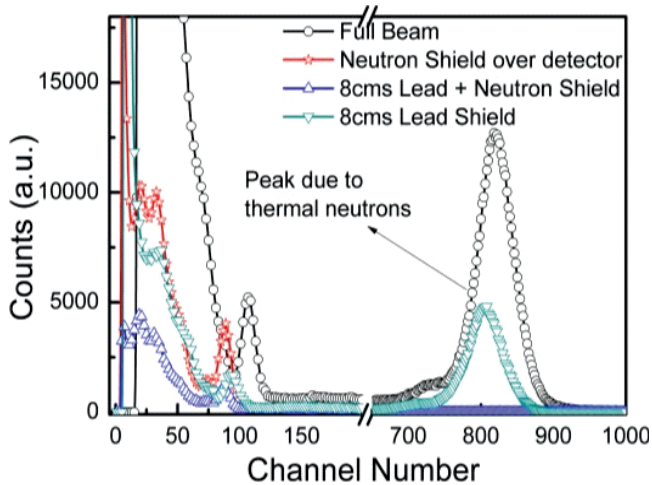
Fig.8: Pulse height spectrum due to thermal neutrons at Dhruva beam line from LiI:Eu^{2+}.

Fig.10: A USB based handheld thermal neutron detector employing LiI:Eu^{2+} single crystal .

the overlap of the transmission and the emission spectrum. The electronic properties needs tailoring to address this issue as large size crystals were required for the higher efficiency and work with co-doing in also in progress.

After studying the optical properties suitable for the scintillation application, the scintillation measurements were carried out on the detectors fabricated from the LiI: Eu^{2+} single crystals. A typical hermetically sealed LiI: Eu detector is shown in Fig.7. The pulse height spectrum originating from thermal neutrons from the Dhruva reactor has been shown in Fig.8. A ^{60}Co source was positioned proximate to the detector to discern the detector's response to both gamma and neutron energies. Notably, the spectra distinctly reveal a prominent peak occurring around channel number 850, attributed to the interaction between thermal neutrons and the ^{6}Li content within the scintillator. This interaction elicits charged particles via the [^{6}Li (n, α) ^{3}H] reaction, inducing scintillation within the crystal. To ascertain the origin of this peak, a borated envelope was employed to enclose the entire detector, leading to a reduction in counts to background levels. A lead shield used in attempt to minimize the gamma background in the reactor hall could also scatter the neutrons and height of the photo peak was found to be reduced but doesn't vanish completely. The photo peaks corresponding to gamma energies of 1.17 MeV and 1.33 MeV originating from the ^{60}Co source were indistinguishable, manifesting at approximately channel number 100. Notably, the scintillator's efficiency for gamma energies was compromised due to its low density and limited effective atomic number (Z_{eff}). However, the scintillator's proficiency in thermal neutron detection exhibited significant enhancement, with the potential for further augmentation through the enrichment of ^{6}Li in comparison to the naturally
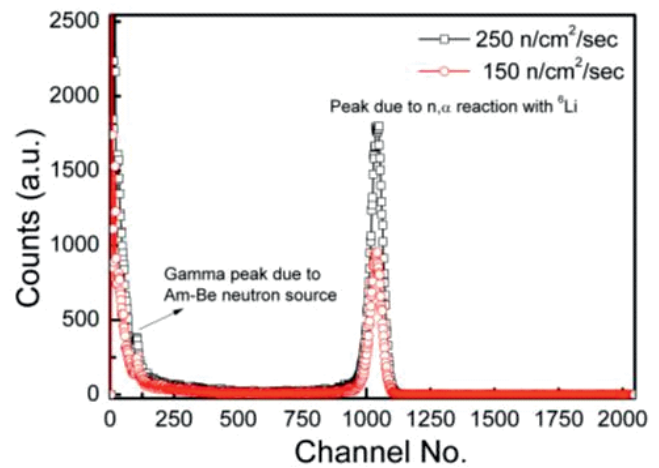
prevalent ^{7}Li. To further understand the linearity response of the LiI: Eu detector, the pulse height measurents at standard neutron flux facility were carried out. The spectrum in Fig.9 shows the response of the detector when radiated with thermal neutrons from the Am-Be Source. The spectrum distinctly portrays a photo peak corresponding to the 4.8 MeV energy deposited by charged particles resulting from their interaction with thermal neutrons. The integrated counts with 150 n/cm^{2}/sec and 250 n/cm^{2}/sec were in good agreement and exhibits the linearity in the response of the neutron flux.

However, the Pulse height spectrum recoded for large size single crystals (2-inch diameter) shows broadening of the peak which may have been originating due to the self-absorption or the impurities affecting the scintillations response of the detector [6,7]. Further experiments are in continuation to improve the detector response for the large size detectors required for the higher efficiency [8].

A hand held detector was designed and developed by CTS, TPD for field application employing the LiI: Eu^{2+} single crystal. A photograph of the detector employing a hermetically sealed LiI: Eu detector is shown is Fig.10. It has been used for long term testing for the stability of the detector over three months. Fig.11 presents the pulse height spectrum acquired from a ^{137}Cs source over a three-month interval, during which uniform signal processing parameters were maintained. Clearly discernible, the spectrum displays a photo peak situated nearly at the same channel, depicting fluctuations below 3%. These slight deviations, possibly stemming from experimental uncertainties, provide substantiation for the reliability of the observed patterns. This underscores the achievement of a secure hermetic seal connecting the scintillator and the directly coupled PMT, thereby ensuring its
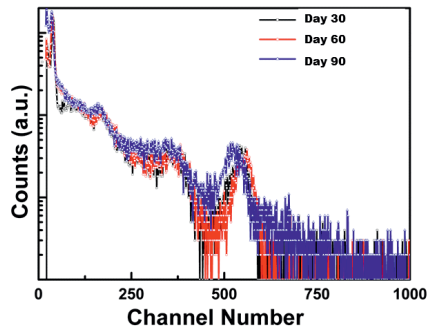
Fig.11: Pulse height spectrum due to ^{137}Cs recoded under identical settings over a period of 3 months.

resilience over an extended timeframe. Concurrently, ongoing inquiries are underway to enhance and optimize the detector's efficiency through the utilization of this hermetic sealing approach.

Conclusion

Single crystals of 0.1 % Eu doped lithium iodide were grown using Bridgman technique. Structural and optical properties show a promising journey towards the development of the high efficiency detectors for thermal neutrons. Detectors fabricated using the LiI: Eu scintillators were used for thermal neutron detection. Thermal Neutron detection has been carried out using the hermetically sealed detector and its long term performance has been evaluated.

References

[1]   G.F. Knoll, Radiation Detection and Measurement, John Wiley & Sons, Second Edition, 1978.

[2]   R. Cervellati and A. Kazimierski, "Wall effect in BF3 counters," Nucl. Instr. and Meth. 60, 173, 1968.

[3]   Sajid Khan, et al, Nucl. Inst. And Meth. A 793 (2015) 31-34.

[4]   Boatner, L.A, et al, Nucl. Inst. And Meth. A 854 (2017) 82-88.

[5]   A.K. Singh et al, Proceedings of the DAE Symp. on Nucl. Phys. 63 (2018).

[6]   Kazuo Suzuki, J. Phys. Soc. Jpn. 10 (1955) 794.

[7]   Kazuo Suzuki, J. Phys. Soc. Jpn. 13 (1958) 179.

[8]   A. Boatnera, E.P. Comera, G.W. Wrightc, J.O. Rameya, R.A. Riedeld, G.E. Jellison Jr., J.A. Kolopusa, Nuclear Instruments and Methods in Physics Research A 854 (2017) 82–88.

Detectors

5

Status of Indigenous Development of HPGe Detectors in BARC

Shreyas Pitale[1], Manoranjan Ghosh[1], S. G. Singh[1], G. D. Patra[1], A. K. Singh[1], M. Sonawane[1], Shashwati Sen[1], R. S. Shastrakar[3], Tushar Kesarkar[3], K. M. Sudheer[3], V. B. Chandratre[3], K. G. Bhushan[2], S. M. Rodrigue[2], S. Malhotra[2], L. M. Pant[1] and S. M. Yusuf[1]*

[1]*Technical Physics Division, Bhabha Atomic Research Centre (BARC), Trombay – 400085, INDIA*
[2]*Electromagnetic Application & Instrumentation Division, Bhabha Atomic Research Centre (BARC), Trombay – 400085, INDIA*
[3]*Electronics Division, Bhabha Atomic Research Centre (BARC), Trombay – 400085, INDIA*
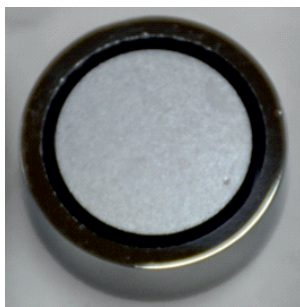
Fabricated diode

ABSTRACT

For the last 5 decades High Purity Germanium (HPGe) Detectors have played key role in nuclear physics experiments and nuclear fuel cycle application in DAE. These detectors are imported in large numbers that are quite expensive and difficult to maintain. A planned program was initiated in DAE in order to develop the technology of HPGe detectors indigenously. The project aims to build gamma ray detectors starting from commercially available raw Ge material, process it by zone refinement to 13 N purity level and grow in-inhouse crystals by Czochralski technique for fabrication of detectors with various configuration and geometries. Currently, P and n-type planar HPGe diodes have been developed by forming suitable electron and hole blocking electrical contacts. A cryostat is developed to maintain the temperature of the detector below 100K and mount the electronics for readout of the HPGe detector. Finally, a complete HPGe detector with indigenous cryostat assembly, readout electronics and software for high resolution spectroscopy are realised which meet the requirements of DAE's activities.

KEYWORDS: *High-purity germanium (HPGe), Czochralski technique*

Introduction

High-purity germanium (HPGe) detectors are preferred in high resolution gamma and x-ray spectroscopy for the identification of closely spaced radionuclides. Compare to silicon, Ge shows high electron and hole mobility, higher atomic number and lower average energy required to create an electron-hole pair. Thus Ge based radiation detectors are best choice for high-energy spectroscopy and no alternatives are found without substantial loss of resolution and efficiency [1].

DAE has been using HPGe detectors for decades in programs ranging from nuclear physics experiments, fuel production to nuclear medicine due to its high energy resolution. These radiation detectors are imported without service support and face export control hurdles. It is the need of the hour that DAE develops the technology to fabricate HPGe detectors indigenously. This project is a step in that direction to mitigate these issues, build capabilities in long run and be self-sufficient.

Basic Principle of HPGe

Most high-energy photons (100 keV–10 MeV) interact with the electrons in the high pure Ge material. The density of electrons is proportional to atomic number (Z). Thus the absorption coefficient and detection efficiency of gamma ray photon is higher for a given volume of high Z germanium. There are three main processes by which gamma rays lose energy in the detecting media: the photoelectric effect, Compton scattering, and e^+-e^- pair creation. The photoelectric process is dominant at low energies (<100 keV approximately) and is related to emission of electrons from the atomic shells. This process depends on the energy of the photons and the atomic number of the detecting media. The energy of a photon is absorbed by an inner-shell electron and leads to its emission from the atom. Subsequently, the photoelectrons lose their kinetic energy in the semiconductor by electron-hole pair generation. In the intermediate energy range, Compton effect dominates, hence the absorption of the photon becomes a multistep process with Compton electrons (<1 MeV) being absorbed after traveling a short distance, while Compton photons are created and absorbed in subsequent steps. Depending upon the size and geometry of the detector, photo-peak can be obtained with high resolution [2].

A planar HPGe detector using a p-type crystal is shown in Fig.1. In this configuration, the electric contacts are created on the two flat surfaces of a germanium crystal. A lithium evaporation and diffusion method is used to form the n$^+$ contact over one of the surface. The thickness of lithium-diffused layer is several hundred micrometer thick. The other
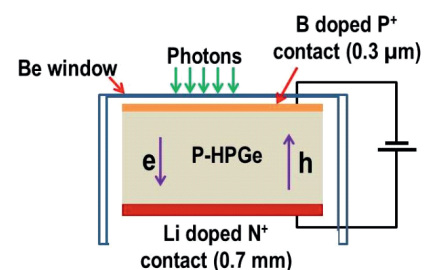
*Author for Correspondence: S. M. Yusuf
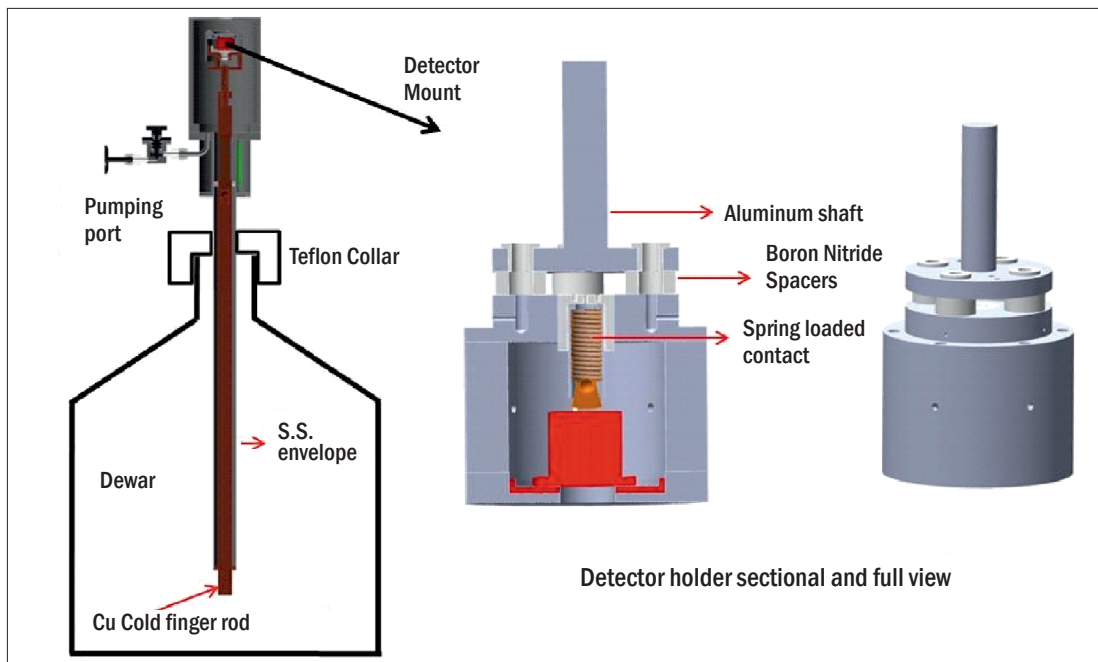*E-mail: smyusuf@barc.gov.in*

Fig.1: Planar HPGe detector (p type).

Fig.2: A complete detector system showing the cryostat and detector holder.

side is 0.3 µm thick boron implanted p^+ layer that provides ohmic electrical contact to collect the charge carriers created by the radiation other wise would be lost in natural recombination process. The depletion region is formed by reverse biasing the p/n junction. The small thickness of the implanted boron layer makes it suitable entrance window for low energy photons. For reverse biasing, a positive high voltage is applied to the n^+ contact with respect to the p^+ surface. The depletion region is formed at the region close to the n^+ contact and then expanded deeply into the p-side as the bias voltage is raised. Once the detector is fully depleted, further increase of the bias (over voltage) does not make any effect on the active volume. However, it makes the electric field stronger, which subsequently shortens carrier collection times and reduces the risk of carrier losses through processes such as recombination and trapping [3].

HPGe crystals were first developed in the mid-1970s. The starting material was chosen as industrial grade germanium. For the purpose of a detector required in high resolution spectroscopy, the material is further purified using zone refining technique. In this process, germanium is melted in a crucible using radio-frequency (RF) heating coils. The underlying principle is that impurities concentrate in the liquid phase leaving the solid purer than the original melt as the liquid freezes and solid appears. As the RF coils are slowly moved along the length of the crucible, the molten zone moves with them. Thus, the germanium melts as the coil approaches and freezes as the coil moves away. The impurities tend to remain in the molten section, which leads to a higher concentration of impurities in the liquid than the solid. In this way, the impurities are swept to one end. This sweeping operation is repeated many times, until the impurities are concentrated at one end of the ingot. This end is then removed, leaving the remaining portion much purer than the original starting material. The improvement or reduction in impurity concentration actually realized is about a factor of 100 or more at the completion of this process [4].

Large single crystals of germanium are grown using the Czochralski technique [5]. A precisely cut seed crystal is dipped into the molten germanium and then withdrawn slowly, while maintaining the temperature of the melt just above the freezing point. The rate of crystal withdrawal and temperature of the melt are adjusted to control the growth of the crystal. The type of conductivity is determined by the donor or acceptor nature of the low-level impurities present in the grown crystal. In order to reach optimum resolution of semiconductor detectors, defect density of the crystal needs to be decreased, in particular for those that are electrically active. In addition to point defects and impurities, dislocations play a major role as they behave like a sink for impurities. This gives a rule of thumb for the dislocation density that should not exceed $10^4 cm^{-2}$ and go below $10^2 cm^{-2}$ for detector-grade material [6].

Because germanium has relatively low band gap, these detectors must be cooled in order to reduce the thermal generation of charge carriers to an acceptable level. Otherwise, leakage current induced noise degrades the energy resolution of the detector [7]. Therefore, HPGe detectors are usually equipped with a cryostat as shown in Fig.2. Germanium crystals mounted within a metal container referred to as the detector holder (indicated in Fig.2) are maintained at temperature 90 to 100 K. The holder is generally made of aluminium and is kept within a vacuum envelope. The detector holder as well as the "end-cap" is thin to avoid attenuation of low energy photons. The HPGe crystal inside the holder is in thermal contact with a Copper metal rod called a cold finger. The cold finger extends past the vacuum boundary into a dewar flask that is filled with liquid nitrogen and transfers heat from the detector assembly to the liquid nitrogen (LN2) reservoir. The combination of the detector holder, vacuum envelope, the cold finger and the liquid nitrogen dewar is called the cryostat. The preamplifier of the germanium detector is normally included as part of the cryostat package and is installed nearest possible distance from the detector to minimize the overall capacitance. The input stages of the preamp are also cooled.

On-going Research in the Field of High purity Germanium Detector at DAE

Owing to its dependence on import for the need of high energy resolution gamma ray detector based on High purity germanium, DAE, under XII plan started a project to

Fig.3: Chemical laboratory in CTL, TPD showing installed fume hoods, water purifier, racks and working table.

indigenously develop the full technology for the fabrication of HPGe detector. The project covers the full technology spectrum including material purification, crystal growth, detector fabrication and readout electronics with spectrum analysis software. For that purpose, well directed and concerted efforts have been put forward towards development of state of the art facilities for the in-house growth of HPGe single crystal and fabrication of detector in Crystal Technology Section of Technical Physics Division, BARC. The readout electronics and software work was undertaken by ED, BARC. A brief description of created facility and ongoing research activity are presented here.

Processing of Ge Crystal for detector fabrication

Well equipped Chemical laboratories (Fig.3) and Ge crystal processing facilities were created for crystal cutting,

cleaning, etching and mechanical polishing. Custom designed holders made of PTFE are used to handle various geometries of crystals during chemical etching. An inventory of high purity semiconductor grade concentrated acids and solvents such as HF, HNO_3, Acetic Acid, Methanol, Acetone, Trichloroethylene, H_2O_2 etc having impurity metal ion concentration (per element) approx. 10-50 ppb and particle concentration < 250/ml, are maintained for chemical treatment of ultra-pure germanium.

The high purity Ge crystal needs to be cut as per the desired size and shapes. A wire saw (Fig.4a) and diamond wheel cutting machines are commissioned for this purpose. A complete process is developed for cutting of the high purity crystals in different geometries. Fig.4 (b-c) shows a high purity Ge single crystal cut in top hat geometry. Also circular grooves were fabricated using a diamond coated core drill bit [Fig.4d] on one face of planer Ge crystal [Fig.4 (e-f)] using SiC slurry mediated core drilling technique. SiC abrasive of grit 220 (particle size ~1000 μm) to 1500 (particle size ~ 10 μm) are used successively to lap the crystal for removal of mechanical damages created while cutting. Further planarization is performed by polishing the crystals with Al_2O_3 powder of particle sizes 9 μm, 3 μm and 0.3 μm. To remove the residual damages created by the polishing process, chemical etching is performed with a mixture of concentrated nitric acid and hydrofluoric acid.

Facilities for qualification of detector grade Ge Crystal

The Ge crystal needs to be characterised before fabrication of gamma detector. A Ge crystal is selected for diode fabrication only if the electrically active impurity is found to be around $\sim 10^{10}/cm^3$, the carrier mobility is higher than 40,000 cm^2/ V. sec, carrier lifetime is higher than 10^{-3} sec and dislocation density is within 3000-7000/cm^2 [8]. Enormous amount of efforts have been devoted to create and maintain facilities, develop the knowhow and expertise for characterization of these critical parameters.
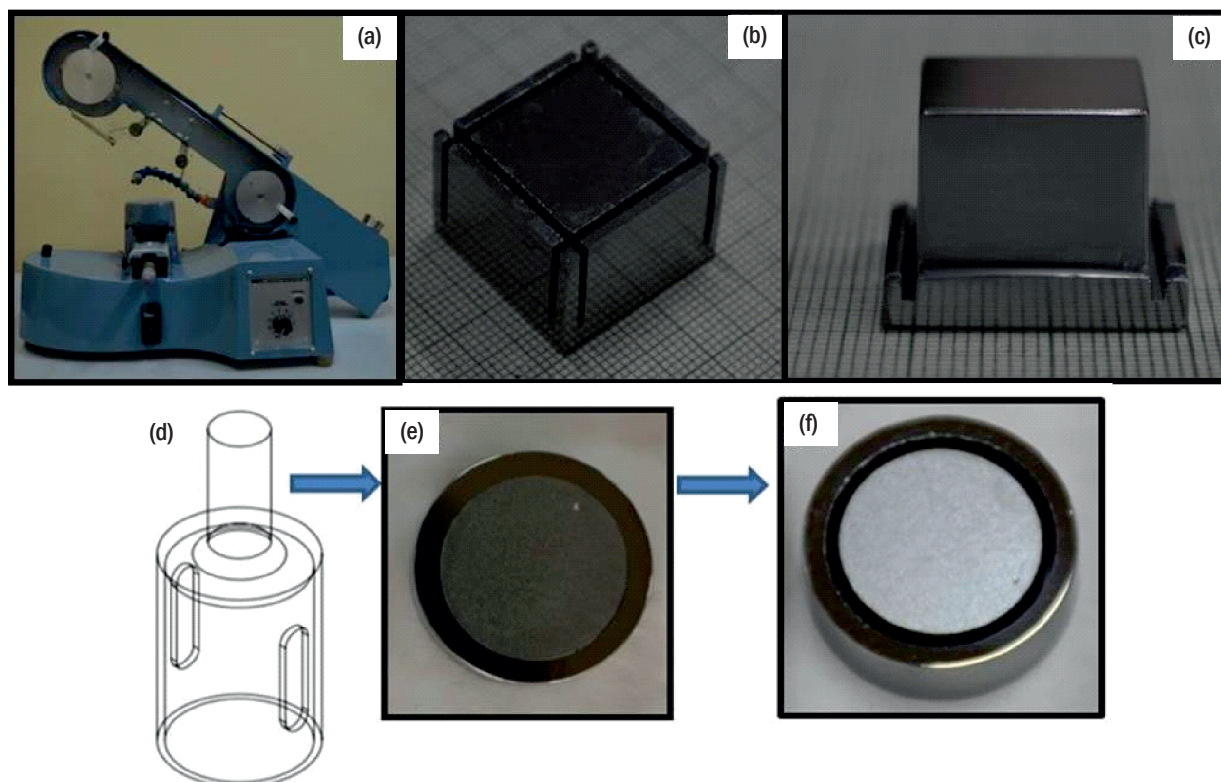

Fig.4: (a) Wire saw cutting machine, (b-c) Crystal processed to various shapes and geometries by cutting and grinding, (d) Schematic of diamond coted core drill bit, (e - f) Circular groove on Ge crystal performed by SiC slurry mediated Core drilling.
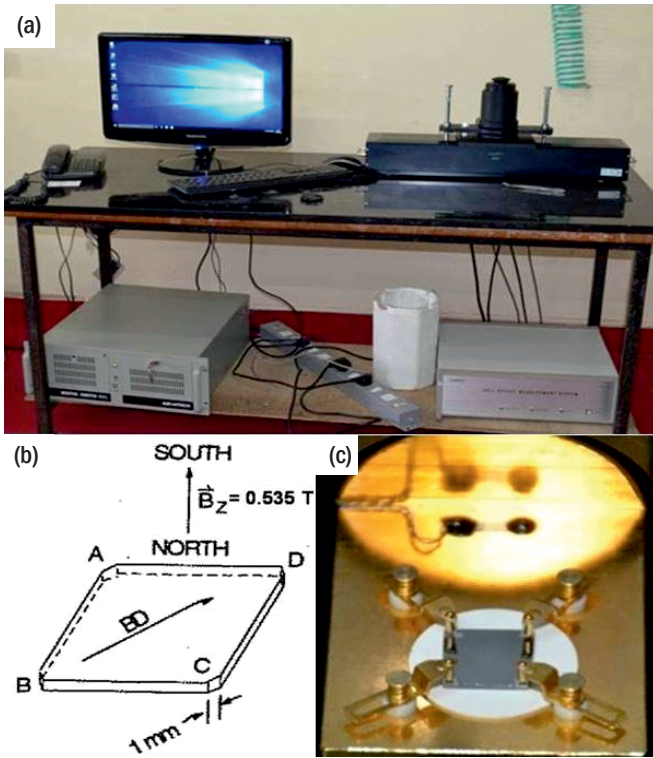
Fig.5: (a) Hall measurement system installed in CTS, TPD (b) Contact arrangement on a square sample and magnetic field for Hall measurement (c) Actual photograph of Ge crystal mounted in four probe configurations on the sample stage.

Facilities for determining crystallinity, dislocation density, band gap and transparency in IR region: Single crystalline nature of Ge crystal is characterized by Laue diffraction and High Resolution X-ray diffraction measurement facilities maintained at CTS, TPD. The optical microscope is used to visualize and measure the etch pit density of Ge crystal exposed by appropriate chemical etching. A Shimadzu make transmission measurement system for wavelength range 180-3000 nm is also used to determine the band gap and transparency in the IR region of grown Ge crystal.

Hall and I-V measurement systems for determining the purity of Ge crystal: Net carrier concentration, mobility and resistivity of the grown as well as procured Ge crystal and zone refined Ge ingot are ascertained in-house following IEEE standard [9] by Hall measurement set up (Fig.5a). The system is equipped with measurement of Hall co-efficient, resistivity, mobility and net carrier concentrations and current-voltage characteristics within the temperature range of 80-350 K. Transport property measurements were carried out in four probe configuration using Van der Pauw method [10]. For this measurement Ecopia make HMS5000 Hall measurement system is employed. IEEE protocol [9] has been followed for sample preparation. Thin Ge sheet of dimension 10 x 10 x 1 mm^3 were prepared from the sliced wafer and were mechanically lapped to a surface finish up to 0.5 micron. Finally the samples were etch-polished using 3:1 HF-HNO$_3$ solution. Four contacts were attached on the corners of polish etched square samples at 90^0 spacing using In-Ga eutectic [Fig. 5(b-c)].

Facility for room temperature collinear sheet resistance measurement has been created that provides first-hand information about the purity of the material. This set up consists of one Keithley make nano-voltmeter, current source and a sample holder with height adjustable four collinear probes. Sheet resistance measurement is found useful for detecting lithium diffusion and boron implantation in Ge.

Transport properties measurement as a function of temperature can give substantial information about the material purity, as the resistivity and mobility show strong dependencies on impurities in a semiconductor material. The carrier concentration (CC) in a semiconductor consists of two parts; (i) intrinsic charge carriers and (ii) extrinsic charge carriers. In an n-type semiconductor, with N_d donor density, the total electron density n can be defined as

$$n = (N_d/2)+[(N_d^2/4)+n_i^2]^{1/2} \qquad (1)$$

$$where \ n_i = (N_v N_c)^{1/2} exp \ (E_g/2k_BT) \qquad (2)$$

$$and \ N_d = N_0 exp \ (-E_g/k_BT) \qquad (3)$$

N_d being the extrinsic carrier density and n_i is intrinsic carrier density, while N_v and N_c are effective density of states of valence and conduction band respectively [11]. Calculated carrier concentration over the temperature range of 78-330K for different extrinsic impurity in Ge is given in Fig.6a.
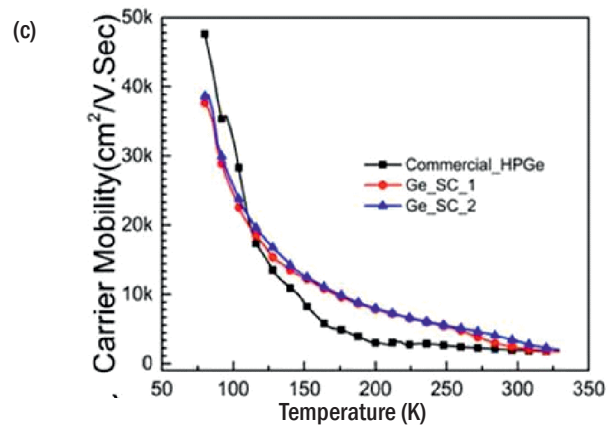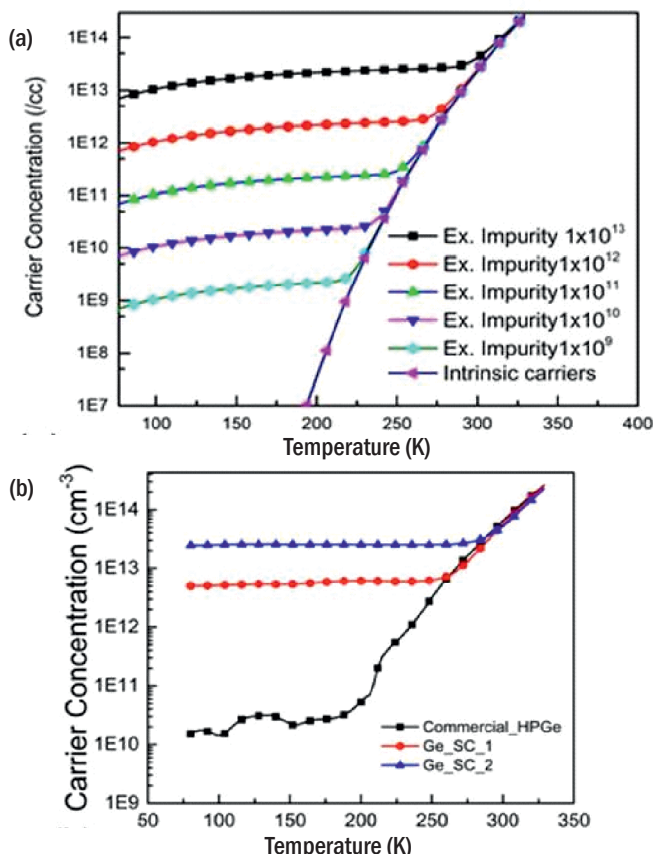

Fig.6: (a) Calculated carrier concentration (eq. 1) profile for different extrinsic bulk carrier concentration (b) Experimentally measured carrier concentration and (c) Carrier mobility of grown crystals (Ge_SC_1 and GE_SC_2) as well as commercial HPGe crystal.
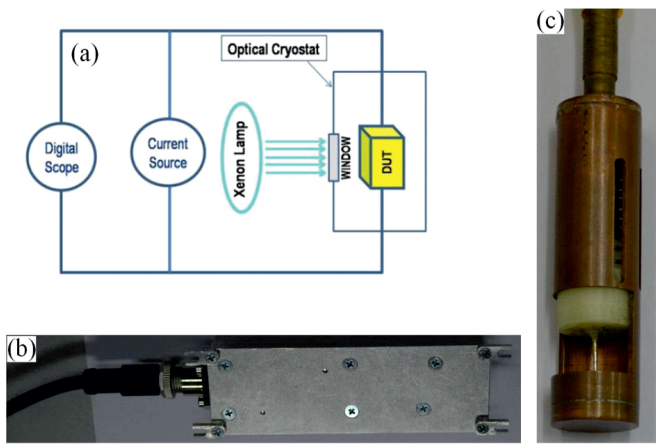
Fig.7: (a) Scheme for determining minority carrier lifetime through decay of voltage pulse after optical excitation of DUT (device under test) (b) IR (1532 nm) pulsed laser source head having repetition frequency as low as 5 Hz procured for excitation of Ge crystal (c) Ge crystal holder fabricated for carrier lifetime measurement by photoconductive decay method.

The surface states in high purity germanium plays an important role in the transport properties measurement as it affects the charge carrier recombination velocity and consequently the carrier mobility measurement [12]. The process for the surface preparation was optimized for the bulk transport properties measurement. The measured bulk carrier concentration of two single crystals grown in CTS, TPD and one commercially procured crystal are shown in Fig.6b which is in good agreement with the theoretically calculated values of carrier concentration for similar extrinsic impurity as shown in Fig.6a. The carrier concentration of the in-house grown crystal is in the range of 5×10^{12} /cc to 5×10^{13} /cc as compared to 2×10^{10} /cc for the commercial HPGe crystal as the in-house grown crystals were 10-12 N pure. The charge carrier mobility as shown in Fig.6c indicates that the mobility of the charge carriers of the grown crystals measured over the temperature range of 78-330 K are approaching the theoretical limit in germanium (~ 50000 cm^2/V. Sec) [13] indicating that the defects are well controlled during growth.

Minority carrier lifetime (MCLT) measurement: The laboratory grown germanium crystal and HPGe (both p and n-type)

crystals are further characterized through Minority Carrier Lifetime (MCLT) measurement using Edinburgh FLP 920 instrument and a Keithley 6221 current source (Fig.7a) as per standard procedure [14]. One IR (1532nm) nano-second pulsed laser source (Fig.7b) is also procured and used as a source for MCLT measurement of Ge crystal. Measurements can be performed both at room temperature and 80 K. The samples mounted in a holder (Fig.7c) are placed in an optical cryostat and excited using pulsed laser or xenon source below 50Hz frequency. Signals were recorded on a Tektronix digital oscilloscope according to the scheme as shown in Fig.7a.

Facilities for in-house fabrication of electrical contacts on high purity Ge crystals

As discussed earlier an HPGe detector is a diode. To fabricate this diode hole blocking (p^+) and electron blocking (n^+) contacts are fabricated on two opposite faces of Ge crystal. Lithium diffusion is conducted for fabricating n^+ contact whereas boron ion implantation is carried out for p^+ contact.

Custom designed thermal evaporation system for lithium evaporation and diffusion

A specially designed thermal evaporation system equipped with a furnace inside the chamber for diffusion of lithium in Ge under Ar environment has been fabricated (Fig.8). The system is capable of depositing lithium on Ge crystal of diameter up to 25 mm followed by thermo-diffusion at 300°C. After the lithium coating is done, the chamber is filled with Argon gas and the crystal can be inserted in a furnace (Fig.8b) to undergo lithium diffusion as per selected diffusion temperature. After the completion of diffusion cycle, the crystal can be retracted out of the furnace and cooled rapidly to room temperature using Argon gas jets shown in Fig.8e to achieve maximum lithium concentration at achieved diffusion depth. Required fixtures for holding Ge crystals, shadow masks and suitable boats are also fabricated. Lithium doped Ge contact (n^+) having sheet resistance below 1Ω at room temperature has been repeatedly formed using this system.

To address the difficulties and challenges of handling lithium in air environment, a Glove Box equipped with thermal evaporation system along with heater (Fig.9) has been installed. The system is found useful for making large area lithium doped n^+ contact on Ge as well as metallization of fabricated contacts.
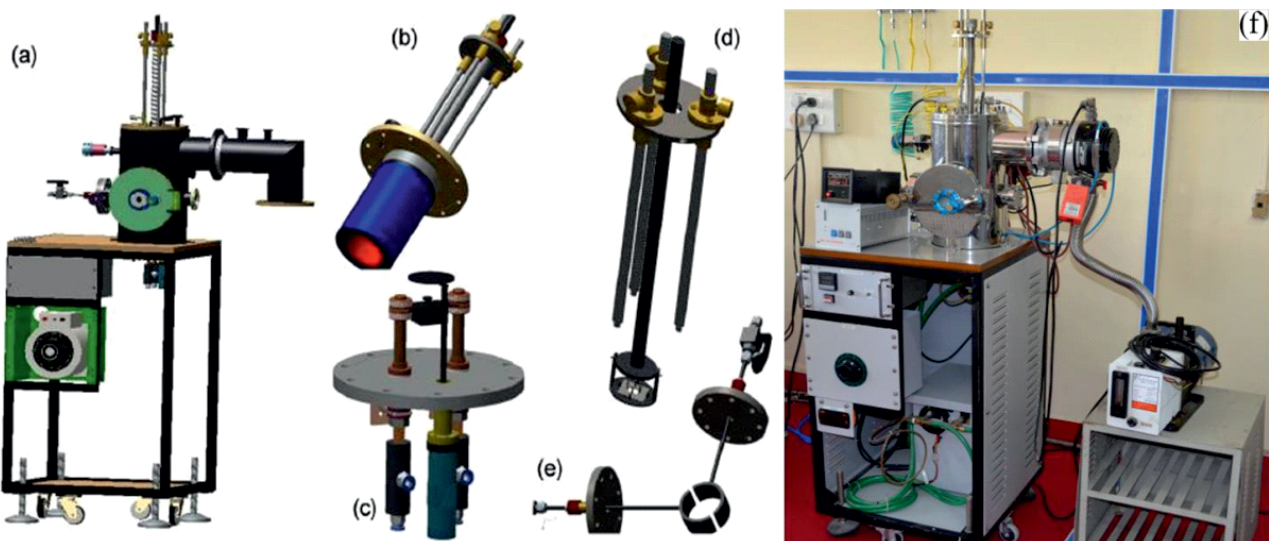

Fig.8: Thermal evaporation system for lithium evaporation and diffusion (a) Completely assembly (b) diffusion heater with sample retracting arrangement (c) Tantalum baffle box source with shutter (d) Sample holder (e) Gas shower jet for rapid cooling after diffusion (f) Actual image of the system installed.

Fig.9: Glove box equipped with thermal evaporation system.

discharge chamber, mass (m/q) selection

current integrator for measuring dose

Sample/target Chamber

Fig.10: Danfysik (1080-30) 30 KeV ion implantation system.

Boron ion implantation system for making p+ contact on Ge: P+ contact is formed by boron ion implantation using the Danfysik (1080-30) ion implantation system (Fig.10). The ion source essentially consists of the discharge chamber and a directly heated oven which is charged with solid substances containing the material to be ionized (BN + B_2O_3 in the present case). A concentrically wound tungsten filament forms the cathode for electrode emission inside the discharge chamber. One positively charged anode ring of tungsten with a central bore is used as an inlet aperture for the source material evaporated in the oven. In the discharge space between the cathode and anode, ions are formed when electrons are emitted from the cathode, i.e., the tungsten filament. The discharge chamber on the cathode side is linked to a tungsten plate having a narrow central bore of about 0.5 mm diameter. Through this bore, the ions are extracted from the ion plasma by means of a highly negatively charged electrode, connected to a potential of at least 10,000 V, and are subsequently fed to the acceleration path and the analysing magnet, respectively. Once extracted, the ions travel through a mass separator where the defined m/q is selected by a sectorial magnetic field. An electrostatic scanning system is used to deflect the ion trajectories. This allows uniform irradiation of the sample (better than 3%) with low current density (of the order of 1 μA cm^{-2}). The implantation is carried out along the [100] direction. The dose is measured by the current integrator, which integrates the current obtained from the four faraday cups.

Surface Passivation and Encapsulation of HPGe diode

The inter-contact region of HPGe diode need to be passivated by chemical treatment followed by dielectric encapsulation for achieving surface leakage current as low as 100 pA at applied field of 1 KV/cm as well as long term stability of the device.

RF sputtering system and required gas supply line: A RF sputtering unit with required accessories along with gas supply line have been set up for deposition of Silicon oxide, amorphous Si, amorphous hydrogenated Ge etc. on the pristine Ge surface (Fig.11). Targets for all required materials have been arranged. The system is easily maintainable and allows quick access to the sample. It is also found useful for making good quality metal contacts showing superior adhesion.

3D Optical Profilometer for measuring film thickness: Thickness of the sputtered deposited and evaporated films are measured by Filmetrics make Profilm 3D Optical Profiler. The system works with the principle of coherence interferometry and provides reliable film thickness in the range of 1 nm to 10 μm.
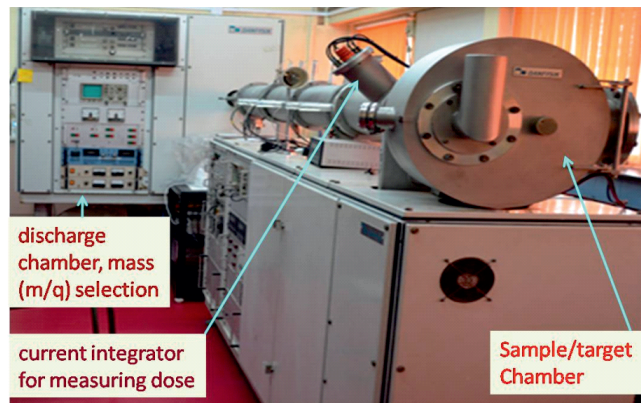
Cryostat for Testing Fabricated HPGe Diode at Near Liquid Nitrogen Temperature

Quick access cryostat for routine current-voltage measurement of HPGe diode: The current voltage measurement of HPGe diode is carried out at temperature nearly 80 K to reduce the population of thermally generated carriers. For relatively quick changeability of devices between successive measurements, a cryostat having shorter temperature cycle is developed in-house (Fig.12a). The basic function of the cryostat is to cool the germanium detector to its near liquid nitrogen operating temperature. The cryostat essentially consists of a double walled hollow chamber containing a solid copper rod. Ceramic to metal sealed high voltage low current vacuum feed through has been used for applying bias and collecting currents. The current path is shielded, ground loops are avoided and cold-end electronics (FET, RC feedback) were embedded(Fig.12b). As per requirements, two such cryostats and specimen holders for maintaining HPGe diode at 80K have been developed. Turbo pump based pumping units are procured for creation of vacuum insulation around liquid nitrogen chambers.

Vacuum envelope with cryo-finger for indigenous HPGE detectors: A liquid nitrogen dipstick is designed and fabricated for housing and maintaining the HPGe crystal near liquid
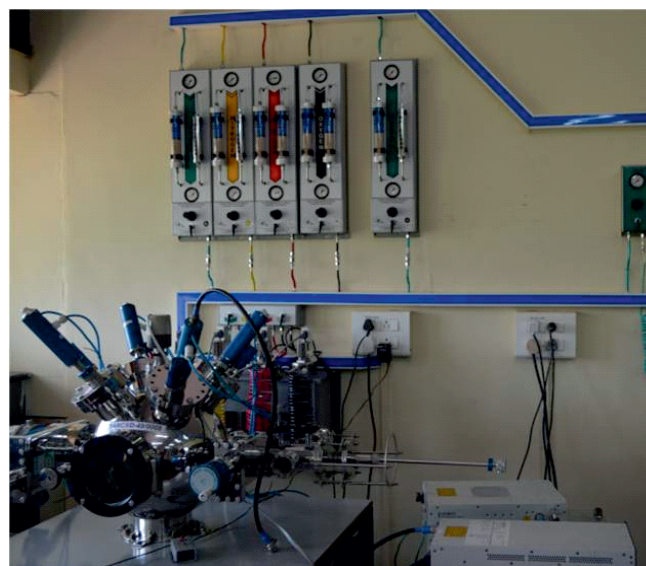
Fig.11: The RF sputtering unit along with gas supply line.

Fig.12: Quick access cryostat for routine current-voltage measurement at 80K (a) Complete assembly (b) Sample mounting arrangement.

Fig.14: Cross sectional view of the planar n-type HPGe diode with grooved structure (left) and actual photograph of fabricated diode (right). .

nitrogen temperature during detector testing (Fig.13a). This consists of fully indigenous construction with multi-pin glass to metal seals having electron beam welding of dissimilar metals and other high vacuum compatible materials such as Zeolites, NEG modules, Vacuum key, etc as shown in Fig.13(b-c). The vacuum envelope allows for high voltage electrical insulation of the crystal while allowing full thermal conductivity to maintain 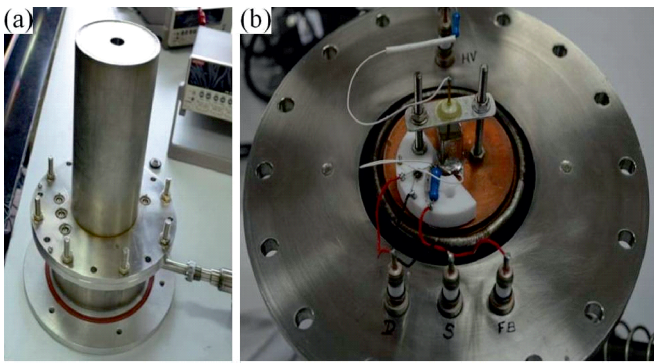the crystal at low temperature. The crystal reaches 88 K and remains at this temperature for at-least 15 days or higher with one fill of LN2 Dewar. No sweating or change in temperature is observed indicating very high vacuum levels maintained in the sealed-off device. A combination of cryo-sorption and NEG (non evaporable getter) pumping modules is implemented to maintains ultrahigh vacuum levels in the sealed off device. Loss of temperature is observed only after LN_2 level falls below half the volume in the container (typically after 3 weeks).

Detector Fabrication and Preliminary Testing

For indigenous development both n-type and p-type HPGe detectors were fabricated and tested. The n-type HPGe detector fabrication started with a cylindrical n-type HPGe monocrystal with the dimensions of 26 mm diameter and 26 mm height. The HPGe crystal was procured from Umicore, Belgium having impurity concentration of 0.85×10^{10} cm^{-3} and 1.2×10^{10} cm^{-3} at the top and bottom planes, respectively. The crystal was cut in to sample of 26 mm diameter and 16 mm length using a diamond impregnated blade saw for further processing. The cut sample was lapped from all side to a surface finish of ~ 10 micron using SiC emery papers of grit size

from 220 to 1500 followed by lapping using 9 micron alumina slurry on a polishing cloth. All the lapping and polishing was done in wet condition to minimize the surface damages during the process. Mechanically processed sample was etch-polished using a solution of HF-HNO_3 mix in 1:3 ratio. Etching time and etchant concentration was optimized to obtain damage free surface. For fabrication of n+ contact (hole blocking), Li was thermally evaporated on one of the flat surface followed by diffusion at 300^0 C for 20 min (Fig.14). To obtain a clean surface and good electrical contact after Li diffusion the crystal was again etched in the 3:1::HNO_3:HF mixture to remove any excess of lithium. After taking Li contact, a 10 mm deep grove of 16 mm ID and 1 mm width was cut in the sample around it using a diamond bonded core drill tool (Fig.14). After fabrication of grove the n+ contact was protected by Apeizon wax and the sample was again etched for 10 min in the 3:1 HNO3:HF solution to remove the mechanical damages on the groove surface. The p+ contact (electron blocking) was created on face opposite to n+ contact by ^{11}B Boron implantation. Danfysik (1080-30) ion implantation system was used for the purpose. The implantation was performed with ions of energy: 25 keV, with dose of 10^{14} ions/cm^2 [15].

Implantation was done at room temperature and no annealing of the sample was performed after implantation [16]. After fabrication, both the contacts were metallized by thermal evaporation of Au (40µg/cm^2). Finally, the sample was etched in a 8:1 HNO_3:HF solution for chemical passivation of the inter-contact surface. After complete process the diode was assembled in a dedicated crystal holder as shown in Fig.2 and integrated with cryostat (Fig.2) for testing detector performance and diode characterization at 100 K.

For fabrication of a p-type HPGe detector a p-type crystal (Umicore Inc., Belgium) having net carrier concentration ≈ 10^{10}/cm^3 was cut using diamond impregnated wheel saw in
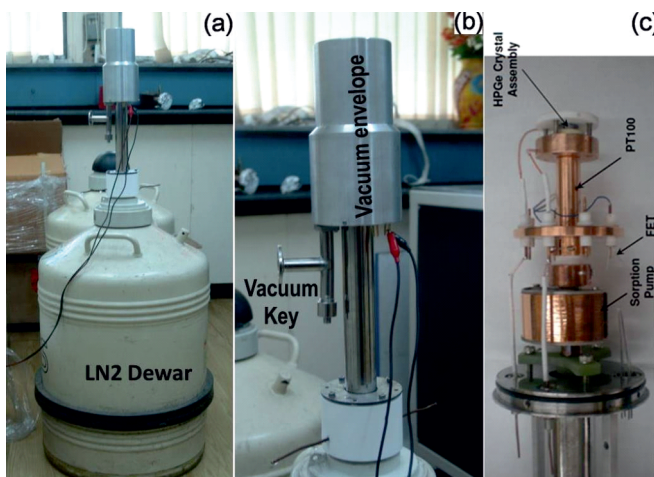

Fig.13: (a) The dipstick cryostat with LN2 dewar (b) The vacuum envelope and (c) Inside assembly of the cryofinger.

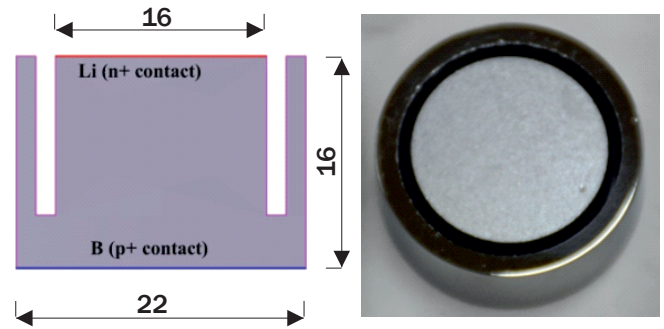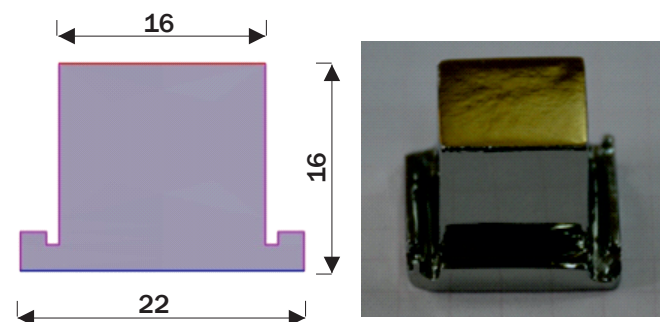Fig.15: Cross sectional view of the planar p-type HPGe diode in top-hat geometry (left) and actual photograph of fabricated diode (right).
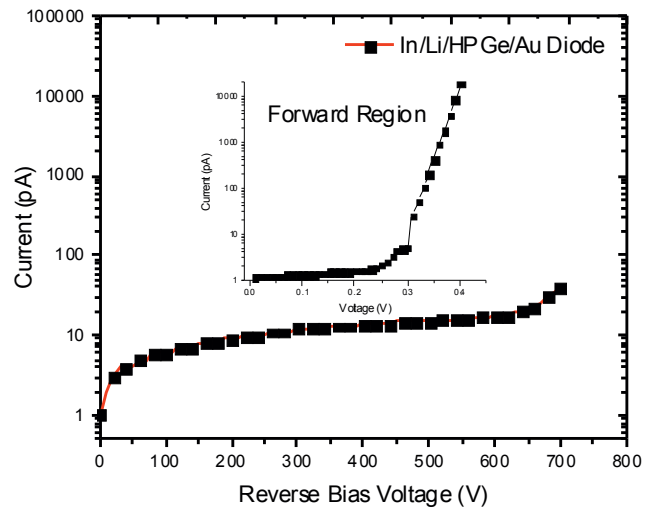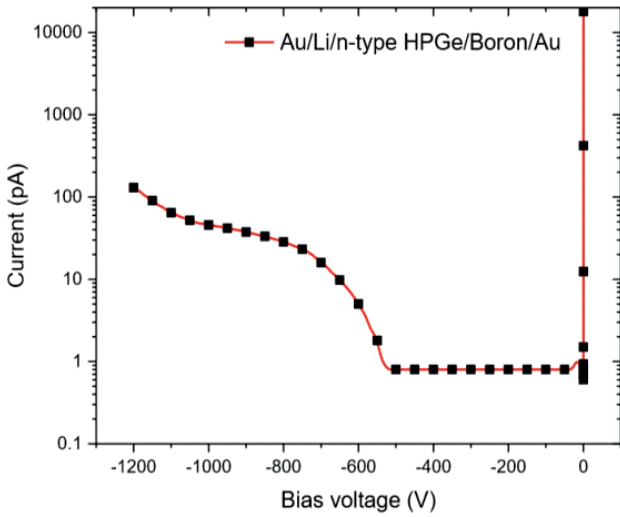
Fig.16: Diode characteristics of n-type (left) and p-type (right) HPGe diode under reverse bias.

top hat geometry (Fig.15). The top hat geometry facilitates crystal handling during various processing steps and also enables the pinching off of surface channels that makes passivation less critical.

The cut sample was lapped from all side to a surface finish of ~10 μm using SiC emery papers of grit size ranging from 220 to 1500 in wet condition to avoid heating related surface damage. Final mechanical surface finish was given by lapping the crystal using 9 μm alumina slurry. Crystals were chemically polished in a solution of $HF:HNO_3$ mixture (1:3) until a smooth damage free surface with mirror finish was obtained. The etch was rapidly quenched in DI water and crystal was rinsed multiple times. n+ rectifying contact was produced by thermal evaporation of Li metal on one of the flat surface followed by diffusion at 300^0C for 15 min in Argon in a custom built thermal evaporation-diffusion chamber as discussed earlier (section 2.3). The base vacuum of the chamber was 5×10^{-6} m barduring lithium deposition. The crystal is cooled within 30 mins to achieve a saturated Li concentration. Diffusion depth and sheet concentration of Li was found to be 250 μm and $10^{17}/cm^3$ respectively [17]. Excess Li was removed by applying methanol and crystal was subjected to 30 sec short etch to achieve a clean lithiated surface.

The lithium contact is masked using etch resistant Apeizon wax and the crystal is subjected to oxidation etch in $HF:H_2O_2$ mixture as described in Ref.[2]. 40μg/cm^2 Au is deposited on the oxidized surface which adheres strongly on the chemically grown oxide layer. Finally, protecting both contacts, the device is etched for 3 mins in $HF:HNO_3$ (1:8) mixture and loaded in a vacuum cryostat cooled to 100 K for leakage current and detection response tests. Current voltage characteristics of the fabricated p and n-type diode were measured at 80 K with an Electrometer. Both the diodes (with

Fig.17: The aluminium crystal holder with the shaft for mounting on the cryo-finger of the dipstick cryostat.
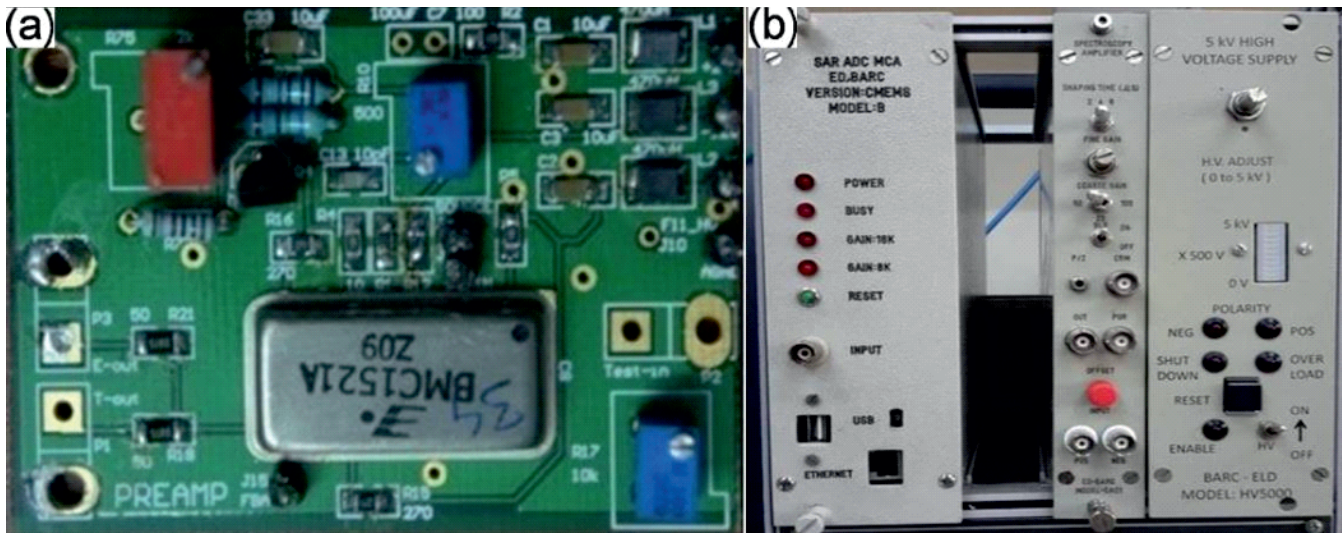
Fig.18: (a) BMC1521 HMC based preamplifier card and (b) NIM based HPGe readout electronics.

Fig.19: (a) 16k portable MCA module and (b) Integrated Multi-channel Analyzer (IMCA).

Fig.20: FWHM resolution of ~1.5 keV @ 661.6 keV Cs-137 peak.

Fig.21: FWHM resolution of ~1.95 keV @ 1332.5 keV Co-60 peak.

n-type and p-type crystal) exhibit less than 100 pA leakage current at 700 volt reverse bias (Fig.16). The forward currents of both diodes increases quickly after the set in voltage around 0.3 V and give rise to high rectification ratio (>10^7). Diodes exhibiting leakage current less than 100 pA at 700 V are selected for detector spectroscopic tests.

For testing the spectroscopic performance of the detector, the fabricated diode is mounted in crystal holder made of aluminium (Fig.17) which is placed on the copper cold finger of the cryostat as shown in Fig.2. Sample holder is designed and fabricated to hold the crystal and apply high voltage reverse bias to it without damaging the diode properties. The materials are suitably selected so that the temperature of the HPGe crystal can be maintained below 90 K when the sample holder is mounted on the cold finger of the dipstick.

HPGe readout electronics & test results

In order to get good resolution from HPGe detector, it is crucial to have readout electronics that has ultra-low noise and high linearity over wide dynamic range. The system noise is systematically minimised by first lowering the noise component in the charge sensitive amplifier (CSA) stage by cryo-cooled input FET and feedback resistor and employing low ripple detector bias, linear low noise spectroscopy amplifier with good Pole-zero (PZ) cancellation & base line restoration (BLR) interfaced to a high resolution nuclear ADC & MCA having good linearity.

Electronics Division (ED), BARC has been involved in indigenous development of electronics for readout of high resolution HPGe detectors. ED has developed BMC1521 HMC
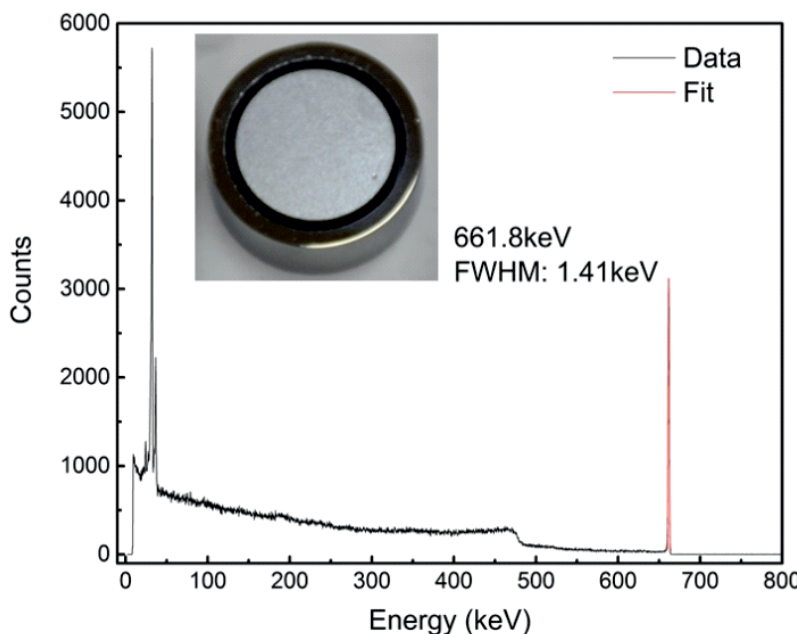
Fig.22: Spectra of ^{137}Cs recorded using HPGe detector (3 cc active volume) fabricated at CTS, TPD employing indigenously made cryostat (EmA&ID) and electronics (ED).

Table 1: Comparison of FWHM of BARC HPGe detector with commercial HPGe detector using lab sources

BARC HPGe - Preamplifier Assembly, p - type, Planar, 3 cc, BARC IMCA/commercial module: HV: +1000 V, Shaping time 6 us, Gain = 30		Commercial (BSI make GCD 50190 p - type, coaxial) HPGe - preamplifier assembly, 50 % efficiency ~ 250 cc, BARC IMCA module: HV: + 2 kV, Gain: 15, Shaping time: 6 µs (RSSD certified)	
Energy (keV)	FWHM (keV)	Energy (keV)	FWHM (keV)
121.5	0.97	121.5	0.916
661.6	1.5	-	-
1332.5	1.95	1332.5	1.835

based low noise compact charge sensitive preamplifier cards (Fig.18a) along with HPGe readout electronics for gamma ray spectroscopy in standard NIM as well as compact bench-top form factors. The instrumentation developed in the HPGe readout chain is: High Voltage bias supply (HV), Spectroscopy Amplifier (SA), 16k Nuclear ADC and Multichannel Analyzer (MCA), in NIM (Fig.18b) and 16k portable SAR ADC MCA (Fig.19a) & Integrated Multi-channel Analyser (IMCA) (Fig.19b) in compact standalone form factors.

The IMCA comprises of HV supply, SA and 16k SAR nuclear ADC, MCA along with LV power supply. The key specifications are: up to ± 5 kV low ripple HV bias supply, SA with selectable shaping time constant (2 µs/6 µs) & adjustable gain (10-150), 16 k fast Nuclear ADC & MCA with INL & DNL of < ± 0.025 % & < ± 1.5 %, respectively and LCD display for continuous monitoring of IMCA parameters like HV value, temperature etc. The IMCA has advanced features like automatic gated Base-line Restorer (Auto BLR), semi-automated PZ assist, automatic HV shutdown & over current protection which are essential for high-resolution gamma spectroscopy. ED has developed ANUSPECT Gamma Spectrum Analysis (GSA) software Package which provides uniform interface to all ED MCA modules through Ethernet.

The BARC p-type HPGe detector & pre-amplifier assembly has been tested with IMCA module. The resolution of ~1.5 keV FWHM at 661.6 keV Cs-137 peak (Fig.20) & ~1.95 keV FWHM at 1332.5 keV Co-60 peak (Fig.21) has been achieved with this indigenous readout electronics. Also, at low energy 32 keV and 36 keV X-ray peaks were well resolved as shown in Fig.22.

Further the detector performance was compared with commercially available HPGe detectors in BARC (Table 1). The results show that the FWHM of the indigenously developed detector is comparable to commercial detectors and can be used for departmental program.

Conclusion

In conclusion, the full know how of the indigenous technology for the fabrication of HPGe detector has been developed in-house. Detector performance was demonstrated and a FWHM of 1.41 KeV with energy resolution of ~0.2 % at 662 keV was achieved. Efforts are going on to increase the detector active volume up to 50 cc with better energy resolution.

References

[1] Kai Vetter, Annu. Rev. Nucl. Part. Sci. 57 (2007) 363–404

[2] J. Ebertha, J. Simpson, Progress in Particle and Nuclear Physics 60 (2008) 283–337

[3] Looker, Q. (2014). PhD Thesis, Fabrication Process Development for High-Purity Germanium Radiation Detectors with Amorphous Semiconductor Contacts, University of California, Berkeley.

[4] Gang Yang, JayeshGovani, Hao Mei, Yutong Guan, Guojian Wang, Mianliang Huang and Dongming Mei, Cryst. Res. Technol. 49 (2014), No. 4, 269–275.

[5] G. Wang, M. Amman, H. Mei, D. Mei, K. Irmscher, Y. Guan, G. Yang, Mater. Sci. Semicond. Process. 2015, 39, 54-60.

[6] E.E. Haller, W.L. Hansen, F.S. Goulding, Proc. of the Mat. Res. Soc. 1982 Annual Meeting, November 1-2, LBL-14916, 1982.

[7] N. Fourches, M. Zielińska, and G. Charles, 'High Purity Germanium: From Gamma-Ray Detection to Dark Matter Subterranean Detectors', Use of Gamma Radiation Techniques in Peaceful Applications. IntechOpen, Oct. 02, 2019. doi: 10.5772/intechopen.82864.

[8] Eugene E. Haller , William L. Hansen & Frederick S. Goulding (1981) Physics of ultra-pure germanium, Advances in Physics, 30:1, 93-138.

[9] IEEE Standard Test Procedures for High-Purity Germanium Crystals for Radiation Detectors," in IEEE Std 1160-1993 , vol., no., pp.1-36, 25 May 1993, doi: 10.1109/IEEESTD.1993.115139.

[10] Oliveira, F.S., Cipriano, R.B., da Silva, F.T. et al. Simple analytical method for determining electrical resistivity and sheet resistance using the van der Pauw procedure. Sci Rep 10, (2020) 16379

[11] Boldrini, Virginia &Maggioni, G. & Carturan, Sara Maria & Raniero, W. & Sgarbossa, Francesco & Milazzo, Ruggero & Napoli, D. & Napolitani, Enrico & Camattari, Riccardo & De Salvador, Davide, Characterization and modeling of thermally-induced doping contaminants in high-purity Germanium, Journal of Physics D: Applied Physics. 52, 3(2018) 035104.

[12] J.P. Ponpon, Nucl. Instrum. Methods Phys. Res., A, 457 (2000), p. 262

[13] C. Claeys, E. Simoen, Extended Defects in Germanium: Fundamental and Technological Aspects, Springer Series in Materials Science, Vol. 118, Springer, Berlin, Heidelberg 2009, Ch. 2, pp. 65–136.

[14] Richard L. Mattis and A. James Baroody, Jr., Carrier Lifetime Measurement by the Photoconductive Decay Method, National Bureau of Standards Technical Note 736 Nat. Bur. Stand. (U.S.), Tech. Note 736, 52 pages (Sept. 1972)

[15] Jones, K.S. & Haller, E. Ion implantation of boron in germanium. Journal of Applied Physics. 61 (1987) 2469 - 2477.

[16] J.P. Ponpon, J.J. Grob, R. Stuck, P. Burger, P. Siffert, Chapter: Boron Implanted Contacts on High Purity Germanium, Ion Implantation in Semiconductors, 1971, ISBN : 978-3-642-80662-9

[17] B. Pratt, F. Friedman, Diffusion of Lithium into Ge and Si, Journal of Applied Physics 37, (1966) 1893–1896.

Scintillation Kinetics through DFT

6

Electronic Structure Analysis to Understand Scintillation Kinetics of CsI Scintillator Single Crystal
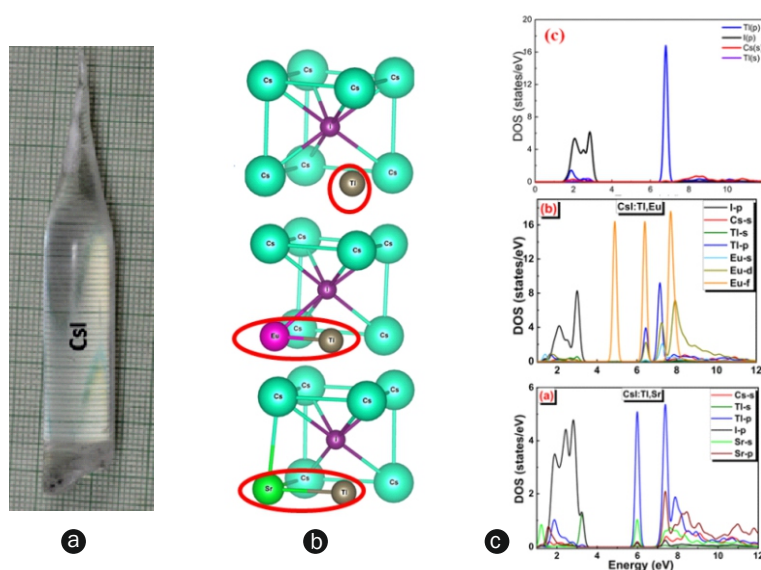
(a) A CsI single crystal developed in BARC.
(b) Local crystal structure of CsI:Tl, CsI:Tl, Eu and CsI:Tl, Sr.
(c) Calculated partial density of states (PDOS) of CsI:Tl (Top) and defect complex and $Tl^-_{Cs}+Eu^+_{Cs}$ (middle) and $Tl^-_{Cs}+Sr^+_{Cs}$ (bottom) in CsI matrix.

Dr. Shashwati Sen is currently heading Crystal Technology Section of Technical Physics Division, BARC. Dr. Sen specializes on the growth of scintillator and semiconductor single crystals for their application in radiation detection. She has more than 200 publications in international peer-reviewed journals. She is the recipient of the DAE Science and Technology Excellence award 2017, DAE-SSPS Young Achievers Award (YAA) in 2008 and DAE Group Achievement award in 2008 for her work on gas sensors, and in 2014, for the growth of single crystals of CsI and NaI for radiation detection applications.

Shashwati Sen
Scientific Officer/G
Technical Physics Division, Physics Group
Bhabha Atomic Research Centre (BARC), Trombay - 400 085, INDIA.

Among the conventional scintillators, CsI:Tl is widely used for gamma spectrometry. Other than having a very high light yield, CsI:Tl has an important ability of differentiating between the incoming radiation based on pulse shape discrimination (PSD). This differentiation arises from the presence of "short" and "long" decay component in the scintillation pulse. Divalent cation co-doping in CsI:Tl are one of the ways of tailoring the electronic structure so as to increase its PSD ability and simultaneously reducing the afterglow.

In a recent study (Sisodiya et al, Optimizing the Scintillation Kinetics of CsI Scintillator Single Crystal by Divalent Cation Doping: Insights from Electronic Structure Analysis and Luminescence Studies, J. Phys. Chem. C, doi.org/10.1021/acs.jpcc.3c06098), experimental investigations along with electronic structure calculations were carried out to understand scintillation kinetics of pure CsI, and doped/co-doped with Tl, Sr and Eu. DFT based electronic structure calculations showed that DX like defect center are formed in the CsI:Tl matrix when co-doped with Sr^{2+} and Eu^{2+} which effects its scintillation kinetics. The study gave an understanding of how the defects need to be tailored to enhance the properties of CsI:Tl.

Applications of Novel Phoswich Detector

7

Assaying of SNM Using Simultaneous Detection of Fission Neutrons & Gamma Rays

(a) Pulse shape discrimination of emitted neutrons and gamma radiation using Phoswich detector.
(b) Measurement of low energy gamma radiation from Pu and Am using Phoswich detector.
(c) Measurement of neutron induced gamma radiation using Phoswich detector.

Mohit Tyagi
Scientific Officer/G
Technical Physics Division, Physics Group
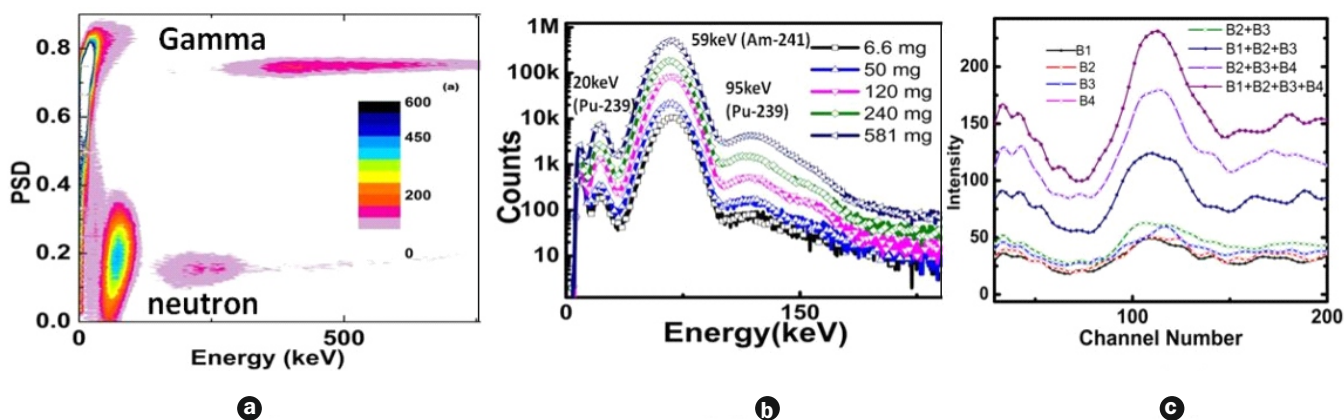Bhabha Atomic Research Centre (BARC), Trombay - 400 085, INDIA.

Dr. Mohit Tyagi joined Crystal Technology Section, TPD in 2005. Dr. Tyagi visited University of Tennessee as Research Associate, and Kyungpook University as Brainpool Fellow. He specializes in the growth and characterization of scintillators for nuclear radiation detection. He has published about 80 papers, and was responsible for 6 patents. He is a recipient of DAE Young Applied Scientist 2014, IACG Young Crystal Grower 2015, IPS Young Physicist 2016, NASI Young Scientist 2017, DAE S&T Excellence Award 2020. Dr. Tyagi is a Young Associate of Maharashtra Science Academy, Core-committee member of Indian Young Academy of Science, and a member of National Academy of Science.

Non-destructive analysis and measurements of the special nuclear materials (SNM) are necessary for various nuclear industries and safeguard applications. Different techniques, like radiation spectroscopy, mass spectroscopy and chemical chromatography etc., have been used to determine the amounts of various SNM (Pu, Am etc.). However, these techniques have the limitations of source phase, strength, age and mixing quantity etc.

In a recent study (Sonu, Mohit tyagi et al., Nuclear Engineering and Technology, 55, 2023, 2662), we have developed a novel phoswich detector consisting of GGAG (front) and CsI (back) single crystals to detect gamma radiation and neutrons from the standard Pu sources very efficiently. Low energy gamma radiation from Pu or Am can be detected and discriminated from high energies and it shows linearity in a wide range of sample quantities. The high specific activity of Am doesn't introduce dead time in CsI as its radiation at 59keV completely stops in the GGAG which has faster decay time. Thermal neutron detection also shows a very good linearity over wide ranges and the quantity of test sample was also calculated accurately by using the measured calibrated plot.

This novel phoswich detector has the potential to detect gamma and neutrons simultaneously and therefore shows more versatile performance characteristics than any other existing systems.

The actual photograph of the developed detector along with the measured (a) Scintillation decay times and discrimination of (b) Gamma-Gamma (c) Alpha-Gamma and (d) Neutron-Gamma radiations.
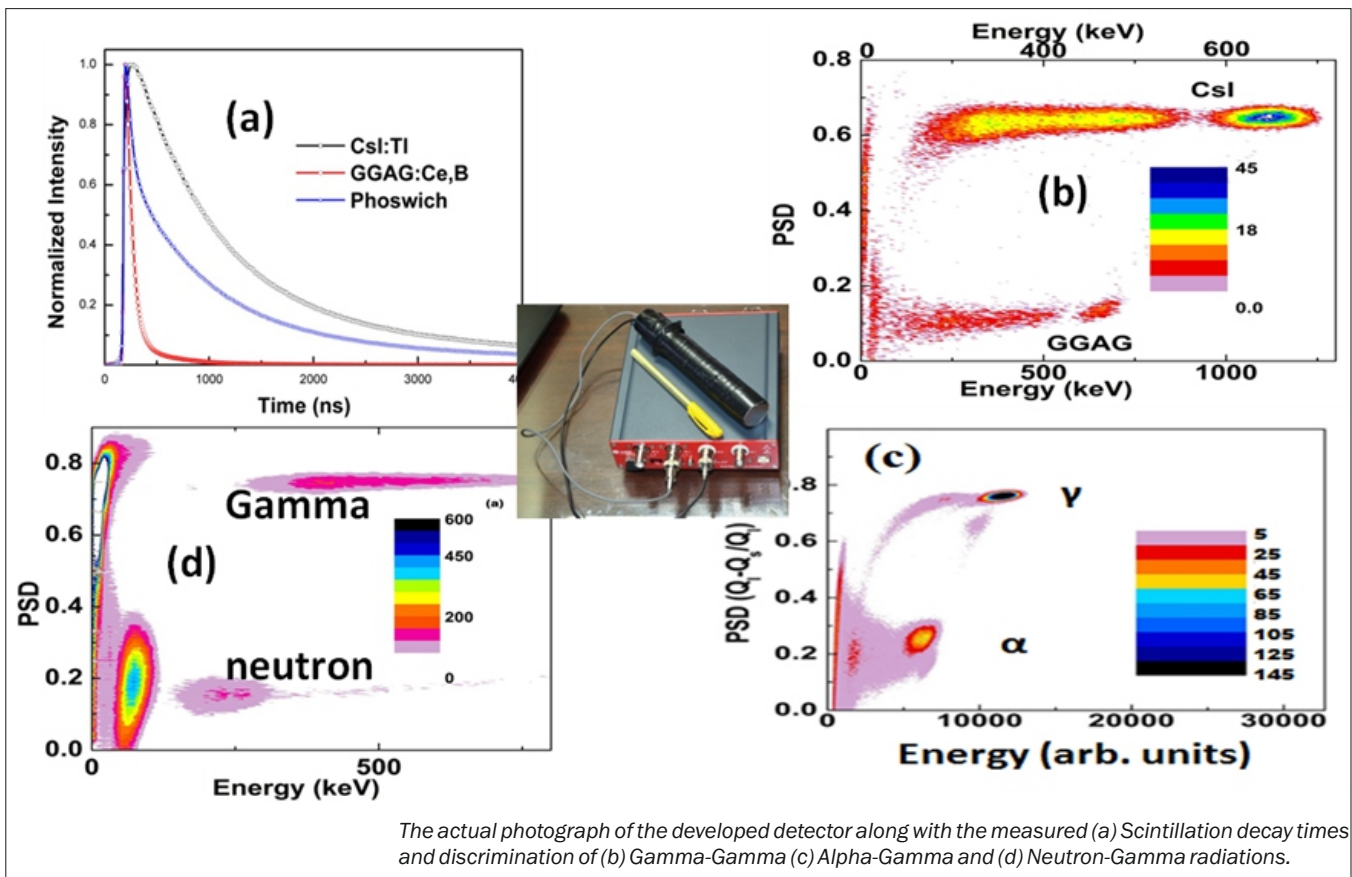
A Novel Versatile Phoswich Detector Consisting of Two Single Crystals to Discriminate Various Kinds of Radiations

*Mohit Tyagi, Sheetal Rawat, S. C. Gadkari

Technical Physics Division, Bhabha Atomic Research Centre, Mumbai 400085, INDIA

This invention was directed to develop a novel phoswich detector consisting of two single crystal scintillators to discriminate various types of radiation elements with high figure of merit and having versatile applications in academic, nuclear, security and medical fields.

Single crystal scintillators emit visible light when exposed to high energy nuclear radiations. The scintillator single crystals have various advantages like high density, high light yield, energy proportionality, high mechanical and radiation hardness etc. when compared to other detectors. For different kinds of radiations like α, β, γ, heavy charged particles, neutrons, etc., different scintillating materials are usually deployed based on the type of interaction, stopping efficiency and conversion into a measurable signal. In a mixed field, different kinds of radiations are usually discriminated by two methods; pulse-height discrimination (PHD) or pulse-shape discrimination (PSD) based on the variations in light-yield or decay kinetics, respectively. The phoswich detectors are sandwich/combination of two or more dissimilar materials with different pulse-shape characteristics and coupled to a common photo-sensor.

Limitations of existing phoswich detectors

The phoswich detectors, reported in the prior inventions and employing gas detectors, organic plastic scintillators, thin films, polycrystalline materials, etc. mainly suffer with the problem of poor efficiencies especially at higher gamma energies. The combination of single crystals has advantage of better efficiency but the difference in refractive indices limits the choice of crystals that could be optically coupled together. Additionally the emission of the first crystal should effectively pass through the transmission region of the second crystal without significant absorption/excitation. Hygroscopic crystals have to be encapsulated and therefore cannot be used for the charged particles. Moreover the detection of thermal neutron requires the presence of atoms having a high thermal neutron capture cross-section that further limits the choice of using single crystals phoswich detectors to discriminate neutrons in addition to charged particles and gamma radiations.

Development of a novel phoswich detector

Single crystals of B co-doped $Gd_{2.98}Ce_{0.02}Ga_3Al_2O_{12}$ (GGAG) and Tl doped CsI were grown by the Czochralski and Bridgman technique respectively. The dopant and co-dopant concentrations were optimized for the best scintillation and discrimination properties. Both crystals have refractive index around 1.9; emit light around 550 nm and have light yield higher about 55000 ph/MeV. The average scintillation decay times are ~ 180 ns and 1900 ns respectively. Very high capture cross-section of the [157]Gd and [155]Gd isotopes and atomic density in the front Gd based garnet crystal stops almost 100% thermal neutrons in a very thin disk of the front crystal while background gamma deposits most of the energies in back halide crystals. The front garnet crystal has ability to discriminate alpha and gamma (X-ray) radiations falling on that. The photo sensor is connected with a desktop based digitizer for generating digital data equivalent to the photo sensor output and discriminating different radiation elements based on pulse-shape discrimination parameter (PSD) corresponds to charges integrated in different time windows corresponding to different radiations.

Novelty of the reported phoswich detector

This novel phoswich combination has the most versatile ability with an enhanced "figure-of-merit" to discriminate different radiations by more than 100% in comparison to that when crystals are used individually. Present phoswich detector also makes it possible to discriminate thermal neutrons due to involvement of the Gd based garnet crystal as the front crystal and the alkali halide single crystal as the back crystal exposed under various kinds of the radiations in a mixed field of neutrons, gamma and the charged particles including alpha particle. It has ability to discriminate incident EM radiation (Gamma, X-rays) radiations that interacted in the front and the back crystals due to the dissimilar pulse-shapes generated through the interactions in one or both the crystals. This is very useful for measuring low energy EM radiation in presence of high energies. Also the gamma interaction with both the front and the back crystals make it possible to measure depth of interaction.

*Author for Correspondence: Mohit Tyagi
E-mail: tyagi@barc.gov.in*

Fig.1: Photograph of (a) Bridgman Crystal Growth Furnace at TPD, BARC. (b) Processed csl:Tl single crystal and (c) A typical radiation detector based on CsI single crystal.

Production and Fabrication of Single Crystals and Radiation Detectors

S. G. Singh, G. D. Patra, D. G. Desai, A. K. Singh, S. C. Gadkari, M Tyagi, M. Sonawane, C. M. More, A. N. Patil, S. S. Revandkar, Shashwati Sen, L. M. Pant and *S. M. Yusuf
Technical Physics Division, Bhabha Atomic Research Centre, Mumbai 400085, INDIA

Cesium Iodide doped with Thalium is one of the oldest scintillator single crystals which finds application in nuclear physics experiments to homeland security and medical diagnostics. This crystal is grown by Bridgman crystal growth technique. In the country this crystal and radiation detector consisting of this crystal is extensively used but till date this is imported. Keeping this in mind and the extensive use in DAE the technology to grow these single crystals and development of radiation detector was developed in TPD, BARC. A system to grow single crystals of CsI:Tl of size 50mm diameter and 75 mm length using Bridgman technique is developed in BARC (Fig.1a). The technology was perfected for the growth of CsI single crystal and growth parameters were optimized. Further processing of the grown crystal and coupling of the crystal to suitable photo-detector to fabricate radiation detector is developed (Fig.1(b) & (c)).

This technology has been transferred to M/s. Electronic Corporation of India, LTD Hyderabad (ECIL) and M/s Ants Systems, Thane in 2018 (Fig.2&3). M/s. ECIL has set up a single crystal growth lab in their premises at Hyderabad and growing CsI:Tl single crystals for commercial applications.

To have a commercial producer of CsI:Tl crystals in India and for development of customized radiation detector the technology was further transferred to M/s. Ace-ex Ltd Mumbai in 2022 and Incubation with the company has been started under Atal Incubation Centre, BARC, from December 2022.

Fig.2: Crystal Growth lab at ECIL.

In the similar note for the growth of oxide single crystals using the Czochralski technique the know-how for the production of oxide single crystals (Al_2O_3, $Y_3Al_5O_{12}$) of 25 mm diameter and 75 mm length was given to M/s. Raana Semiconductors, Hosur. The technology to grow the YAG and sapphire single crystals has been given so that commercial production of these crystals can be started in the country. In addition the technology to develop Czochralski Crystal growth Puller has also been shared under the technology transfer so that the company can develop the pullers indigenously with an aim towards 'Atma Nirbhar' Bharat in the field of Single Crystal growth for various applications.

Fig.3: Incubation Agreement signed with M/s. Ace Ex Pvt. Ltd., Mumbai on Dec. 22, 2022.

Technology Transfer agreement signed with M/s. ANTS.

*Author for Correspondence: Dr. S. M. Yusuf
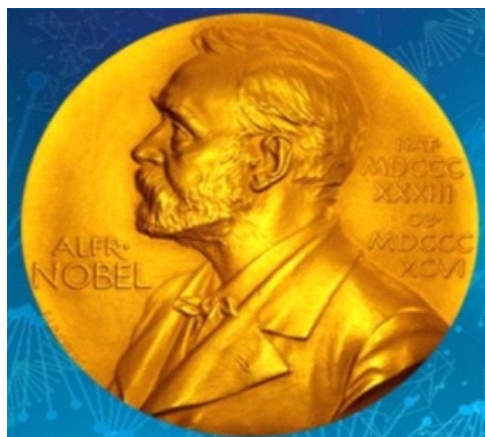E-mail: smyusuf@barc.gov.in*

2023
Nobel Prizes in Sciences
Physics, Chemistry and Physiology & Medicine

Photo courtesy: Official website of Noble Prize Association

Compiled by:
Dr. B.K. Sapra, Head, Radiological Physics and Advisory Division, BARC (bsapra@barc.gov.in)
Dr. Bhushan Dhabekar, Radiological Physics and Advisory Division, BARC, Mumbai (dbhushan@barc.gov.in)
Dr. Pallavi Singhal, Health Physics Division, BARC (psinghal@barc.gov.in)
Dr. Rajesh K. Chaurasia, Radiological Physics and Advisory Division, BARC (rajeshc@barc.gov.in)

Nobel Prize in Physics: Peering into the Microcosmos - Attosecond Science

Photos courtesy: Official website of Noble Prize Association

Anne L'Huillier Pierre Agostini Ferenc Krausz

The 2023 Nobel Prize in Physics has been awarded to three scientists for groundbreaking work in "experimental methods that generate attosecond (as) pulses of light for the study of electron dynamics in matter". These attosecond pulses serve as a potent tool, functioning like a powerful microscope on a time scale, enabling the study of electron dynamics in matter.

The time scales associated with various ultra-fast processes

Fig.1 depicts the time scales involved in different ultra-fast processes. Mechanical shutters and "microwave electronics" equipped with fast transistors are capable of probing processes up to ~ns, while delving into smaller time scales requires "ultra-fast optics" and "light-wave electronics" facilitated by laser technology.

Fig. 2 showcases the evolution of laser technology with respect to pulse duration and peak power. In 1960, the continuous wave laser was invented. Shortly thereafter, short-duration pulses with high power were generated for applications like laser ablation, laser cutting, and drilling. The discovery of the Q-switching technique in 1962 allowed the generation of pulses of ~ns with peak power reaching ~GW/cm^2. In 1964, the development of the mode-locking technique enabled the generation of ~ps pulses with peak power ~TW/cm^2. After a hiatus of 20 years, in 1985, the advancement to the Chirped Pulse Amplification (CPA) technique allowed the generation of femtosecond (fs) pulses with power generation of PW/cm^2 without causing damage to the gain medium. Ahmed Zewail received the Nobel Prize in 1999 for utilizing fs lasers to study the motion of atoms in molecules. This set the stage for the production of attosecond (as) pulses using the peta watt fs laser.
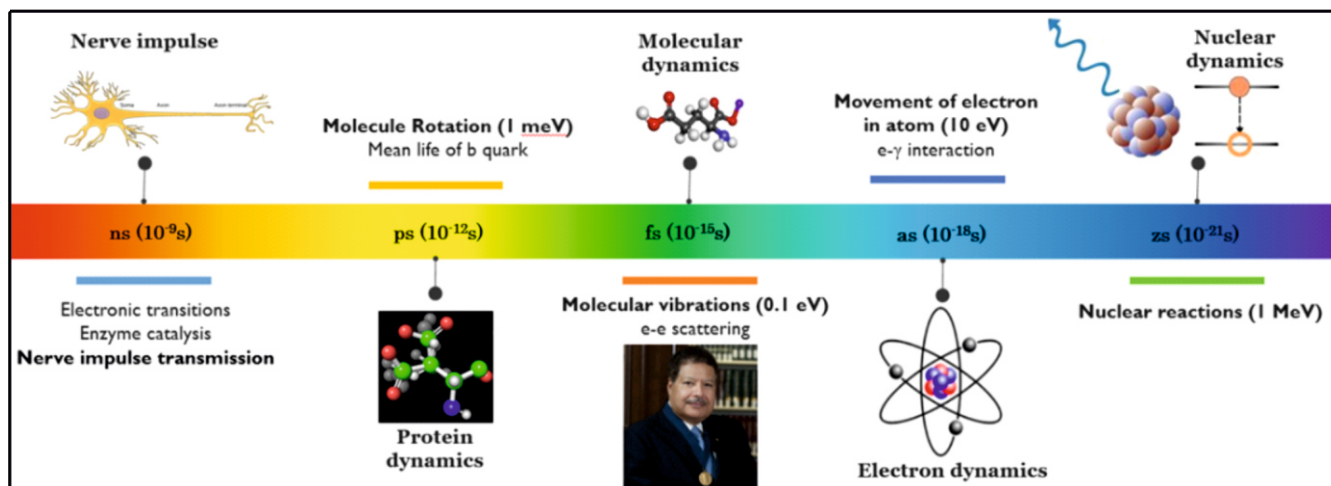

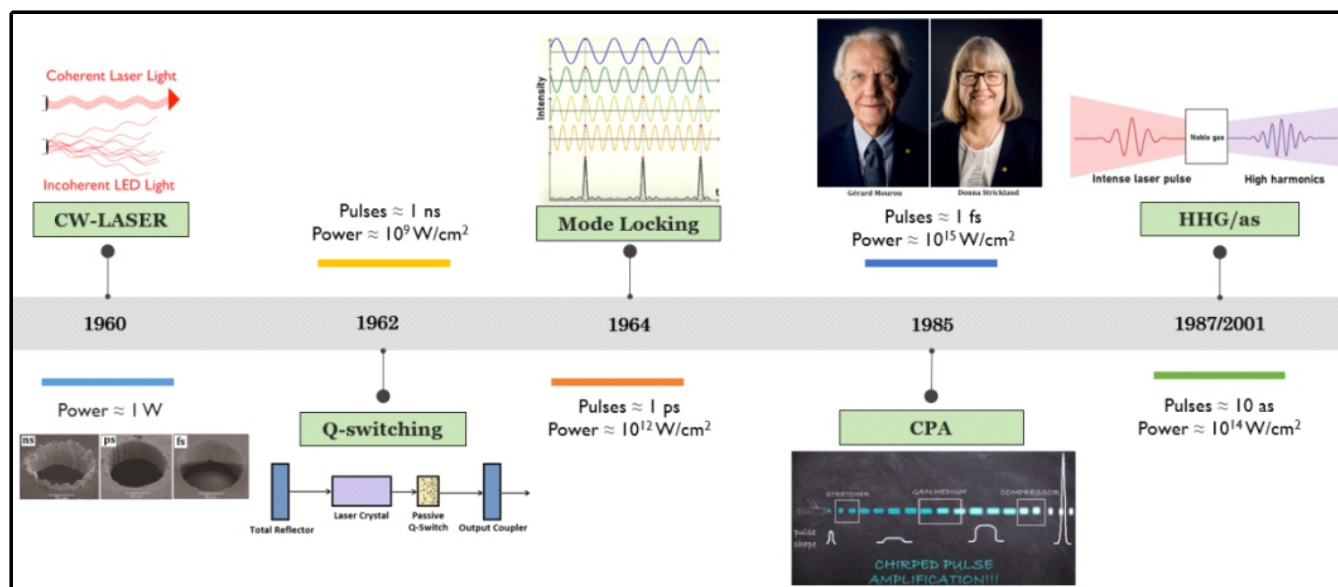*Fig.1: Time scales involved in various processes.*

Fig.2: Evolution of laser technology.

Challenges to produce as pulses

The primary limitation lies in the optical time period of light, restricting the pulse duration. Use of a Ti-sapphire laser directly (λ ~ 800 nm, T ~ 2.7 fs), will lead to generation of pulses of only about 3 fs. Thus, the initial step in generating an *as* pulse involves producing coherent XUV (extreme ultraviolet) radiation (λ ~ 30 nm, T ~ 100 as). One method for generating XUV radiation is through Free Electron Lasers (FEL). However, the drawback is that FELs necessitate kilometer-long accelerators, making them impractical for conventional laboratory work. In the 1980s, Anne L'Hullier and her research group conducted experiments and directed a high-power infrared (Ti-Sapphire) laser onto Argon gas. They observed that the output not only included the original light, but also photons of higher frequencies, that were odd integer multiples of the incoming photon frequency. Thus, exposing noble gases to a high-power red laser with a photon energy of about 1eV, photons of higher energies, reaching up to hundreds of eV, were generated. This phenomenon is referred to as High Harmonic Generation (HHG).

Mechanism behind HHG

Paul Corkum from Canada, a significant contributor to theoretical attosecond physics, proposed a three-step classical process to explain HHG. Despite his notable contributions, he has not been included in the Nobel list. Fig. 3 (a) illustrates the Coulomb potential experienced by an electron in a noble gas. The electron is initially trapped within the atom due to the barrier height of the Coulomb potential.

When a laser field, ~peta W/cm^2, is applied to the noble gas, the laser electric field becomes comparable to the Coulomb field, distorting the latter entirely (Fig.3 (b)). This distortion reduces the height of the Coulomb barrier, enabling the electron to tunnel through the barrier quantum mechanically (Fig. 3 (c)). This constitutes the first step of the process. In the second step, the electron undergoes acceleration (by absorbing multiple photons), moving away from the ion to a distance of up to tens of angstroms, gaining significant kinetic energy (Fig. 3 (d)). Subsequently, as the last step, the electric field of the laser reverses, prompting the electron to travel back towards the ion and undergo a re-collision, thus releasing the kinetic energy gained in the second step by emitting a photon. The energy of the emitted photon depends on the phase of the driving laser at the time of electron tunneling and can be as high as a few 100 eV (Fig. 3 (e)). It is to be noted that these photons are produced only during a fraction of time period of the driving laser, when the electric field is high enough.

Fig.3. Mechanism to explain HHG (a) potential experienced by an electron in noble gas atom (b) distortion of the Coulomb potential due to high power driving laser, which leads to tunneling of the electron (c) acceleration of the electron away from the parent atom (d) the electric field of the driving laser reverses pulling the electrons back. (e) re-collision of the electron giving rise to emission of photons extending up to XUV region. In effect, when a high-power laser with a pulse width of approximately 3 fs and a photon energy of around 1.5 eV is incident on noble gas, high harmonic generation allows generation of photon pulses lasting approximately 100s of as, with a photon energy of approximately 100 eV (Fig. (4)).
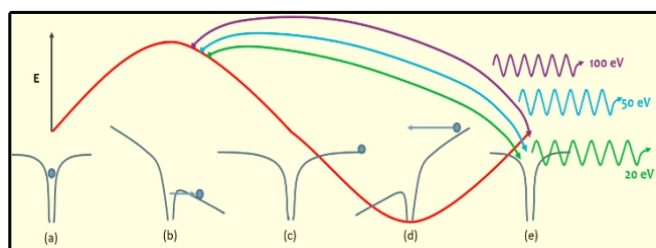

Fig.3: Mechanism to explain HHG (a) potential experienced by an electron in noble gas atom (b) distortion of the Coulomb potential due to high power driving laser, which leads to tunneling of the electron (c) acceleration of the electron away from the parent atom (d) the electric field of the driving laser reverses pulling the electrons back. (e) re-collision of the electron giving rise to emission of photons extending up to XUV region.
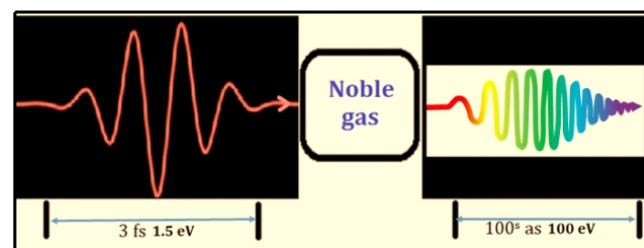

Fig.4: Ti-sapphire laser (λ ~ 800 nm, T ~ 3 fs), when directed on noble gas, produces photons with energies up to 100 s of eV. These photons are produced only during a fraction of the time period of the driving laser, when the electric field is high enough. Thus, the burst of high energy photon lasts only up to 100s of as.
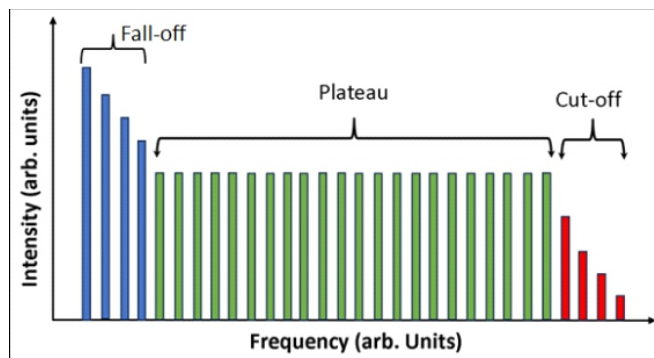
Fig.5: A generic HHG spectrum with its characteristic features:initial intensity fall-off, plateau and the cut-off.

From quantum mechanical perspective, the electron tunnelling can be conceptualised as a beam splitter for the wave function. It divides a bound-state electron wave packet into two: one remains in the bound potential, and the other propagates in the ionization continuum. The coherently re-colliding electron wave packet interferes with the bound-state electron wave function, resulting in a dipole that produces coherent light in a short burst of radiation extending into the XUV (extreme ultraviolet). This technique is truly unique in nature, offering a time scale resolution of approximately 100 as and a spatial resolution of around 1Å.
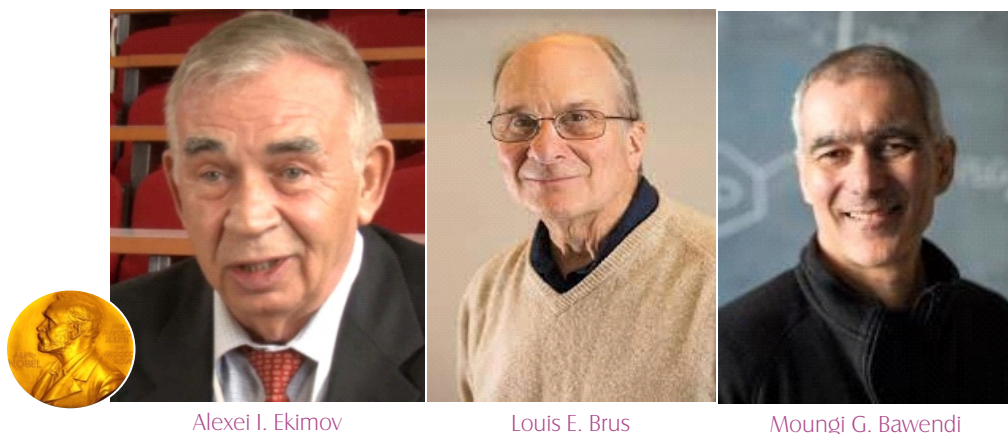
Contributions of each Nobel laureate

In the 1980s, Anne L'Huillier studied phenomenon of HHG and in 1991,presented the shape of the HHG spectrum through numerical solution of the time-dependent Schrödinger equation (Fig.5). It was realised that HHG is a single electron effect, providing the first ever discussion of macroscopic phase matching, which required solving Maxwell's equations. In 2001, Pierre Agostini created a train of pulses, each of 250 as duration and invented the Reconstruction of Attosecond Beating by Interference of Two-photon Transitions (RABBITT) technique to characterize the as pulses. To address the requirement of isolated pulses, such as in pump-probe method, FerencKrausz, in 2001, successfully separated individual ultrashort pulses from a pulse train. These isolated pulses, with a duration of 650 at to seconds, became instrumental in the study of electron dynamics.

Applications of *as* physics

Electrons are in the heart of most of the processes in physics, chemistry, biology and electronics, and hence knowing the motion of electrons enables a better insight into its applications and control. For example, as pulses allow to study ultrafast processes within molecules, such as electron dynamics during chemical reactions. They enable the investigation of electronic structure and dynamics in matter, providing a tool for attosecond spectroscopy. Inpump-probe experiments, *as* pulses are used in to investigate processes like electron tunneling and ionization on extremely short timescales that has applications in time-resolved imaging, and capturing snapshots of ultrafast processes in materials. When applied to study the ultrafast dynamics of biomolecules, *as* techniques can provide insights into biological processes. This is useful for understanding the working principle of medicines in human body, with a possibility of tweaking the medicines for enhancing their potential.

Nobel Prize in Chemistry: Discovery and Synthesis of Quantum Dots

Alexei I. Ekimov   Louis E. Brus   Moungi G. Bawendi

Photos courtesy: Official website of Noble Prize Association

The 2023 Nobel Prize in Chemistry was awarded to three scientists, Alexi I. Eklimov (Nanocrystals Technology Inc., New York, NY, USA), Louis E. Brus (Columbia University, New York, NY, USA) and Moungi G. Bawendi (Massachusetts Institute of Technology (MIT), Cambridge, MA, USA) for the "Discovery and Synthesis of Quantum Dots".

Quantum Confinement

Quantum Dots (QDs) are semiconductor nanocrystals which show "quantum confinement effect", which manifests when the size of the particle becomes comparable or smaller to the natural length scale of electron and hole. This natural length scale is known as Bohr radius. When the particle size is less than the Bohr radius, the color changes with change in the dimensions and is given by the equation 1:

$$E_g(QD) = E_{g,0} + \frac{h^2}{8m_{eh}R^2} \qquad (1)$$

where, $E_{g,0}$ is the band gap of bulk semiconductor. $E_g(QD)$ is the band gap of QDs having radius R. m_{eh} is the reduced mass. It is interesting to observe from eq. 1 that band gap of a material increases with decrease in size. Although, this relationship was known in 1980s, it had not been practically demonstrated. On the other hand, the utilization of this effect was very well done by our ancestors in Lycurgus cup, Abbasid tiles and Medieval church windows.

With the development of molecular beam epitaxy, researchers have shown that the formation of a thin film of nanomaterials over a surface, changes color with change in size, thus practically verifying the size - band gap relationship.

Quantum Confinement Effect in Glasses

Alexi I. Eklimov was not very satisfied with the molecular beam epitaxy approach on quantum confinement is explanation, since it needed extremely low temperatures and ultrahigh vacuum, both of which were unlikely in ancient times. Thus he started reinventing the mystery and initiated work in this direction. He was a semiconductor scientist working in Russia and was familiar with the power of optical techniques in understanding material properties. He began investigating glass formation process for which he doped 1% CuCl in fused silica and heated it at different temperatures for different times. He monitored that the CuCl crystals were formed inside the glass, the size of which was determined using small angle X-ray scattering. He then observed that the optical absorption spectra of the glass changes with change in size of the particles. This was the first experiment that practically showed that the size of particle is related with its size. He then carried out systematic studies and showed that at high temperatures and for longer heating durations, particles size increases, thus unfolding the mystery behind the colored glasses. However, his research was not very well documented in open literature and here comes the contribution of other Nobel laureate Louis E. Brus.

Demonstration of Size Quantization in Solutions

Louis E. Brus was working in Bell laboratories as a catalyst scientist. He was the first scientist to demonstrate that the size quantization effect can also occur in free flowing solutions. His research was focused on harvesting solar radiation for chemical reactions, for which he was using CdS nanomaterials as a catalyst. In one instance, he observed that the color of the CdS nanomaterials solution changed when left overnight. He was fascinated by this behavior and then started exploring it much deeply. He measured the absorption spectra and size of both fresh and aged particles and observed that the spectra shifted towards red in aged particles as compared to fresh ones and also the size was larger in aged particles as compared to fresh ones. He then carried out more systematic studies and synthesized different size particles in two different solvents, water and acetonitrile to study the effect of solvent on size and aging. It was observed that the large size particles have red shifted absorption spectra as compared to small size particles and the average size is less in acetonitrile as compared to water. The results were found to correlate with size quantization effect. Brus was the first scientist in the world to show that the size quantization effect in particles is practically possible.

Synthesis of High Quality Quantum Dots

Moungi G. Bawendi was the third Nobel laureate in the series. He developed a method to synthesize high quality, reproducible and monodisperse QDs. He was the post doctoral student of Louis E. Brus at Bell laboratories, where he was working on the synthesis of monodisperse quantum dots. However, he did not succeed until he moved to Massachusetts Institute of Technology (MIT). Here he developed a method to synthesize high luminescent QDs by hot injection route. For the synthesis, he employed organometallic Cd precursor in TOPO as a solvent and TOPX (X- S, Se, Te) as chalcogenide source. The reaction was carried out at 280-300 °C and depending on injection temperature, reaction time, and concentration of precursor different size particles were synthesized. The particle size was measured by TEM and corresponding absorption spectra were recorded. It was observed that the absorption spectra of the particles shifted towards red wavelength as the particle size increases. This procedure of high quality QDs synthesis has opened many areas of application of QDs such as in LEDs, solar energy harvesting, sensing and in diagnosis for which Bawendi was awarded the Nobel prize.

Nobel Prize in Physiology and Medicine
For development of mRNA vaccine against COVID-19

Photos courtesy: University of Pennsylvania, Philadelphia, USA & Official website of Noble Prize Association

Dr. Katalin Kariko (Hungary)
(RNA Biochemist)

Dr. Drew Weissman (USA)
(Immunologist)

The 2023 Nobel Prize in Physiology or Medicine was jointly awarded to Katalin Karikó and Drew Weissman for their groundbreaking discoveries in nucleoside base modifications, which catalyzed the development of highly effective mRNA vaccines against COVID-19. This article explores how conventional vaccines are usually made, the difficulties in traditional vaccine development, the exciting beginning of mRNA vaccines, and how Karikó and Weissman changed medicine with their great ideas.

The Evolution of Vaccines

To understand why Karikó and Weissman's work is important, it is important to understand the conventional methods of developing vaccines. In the past, vaccines were created using either the weakened or whole viruses or bacteria that were responsible for causing a given disease. Examples of such vaccines include those for polio, measles, and yellow fever. As science advanced, researchers started making

vaccines by using specific parts of the viruses instead of the whole virus. This approach paved the way for vaccines against diseases like hepatitis B and human papillomavirus. Some vaccines even use harmless viruses to carry parts of the harmful ones, like in the case of Ebola.

The work of Karikó and Weissman added a new dimension to the story by using mRNA to make vaccines. This is like a set of instructions that helps human cells create proteins. Before their discovery, using mRNA was tricky because it caused inflammation and was not stable. But, Karikó and Weissman figured out how to modify the mRNA so as to eliminate these issues.

In simple terms, they made a breakthrough in finding a better and faster way to make vaccines using the instructions in our cells, and this has been a big deal, especially during the COVID-19 pandemic.

Modus-operandi of vaccines

Vaccines work by leveraging the body's immune response mechanisms, particularly the adaptive immune system. They typically contain weakened or inactivated forms of pathogens, their proteins, or genetic material. When a vaccine is administered, these components mimic the presence of the actual pathogen, prompting the immune system to mount a defensive response. Following steps takes place after administration of vaccine inside the human body.

The immune system recognizes the foreign elements in the vaccine as antigens. Antigens are substances that provoke an immune response. This recognition triggers the activation of immune cells, such as macrophages and dendritic cells.

Immune cells present the antigens to specialized cells called T cells and B cells. This process educates these cells about the specific characteristics of the pathogen, enabling them to respond effectively.

T cells play a crucial role in coordinating the immune response. They can stimulate other immune cells, like B cells, and directly attack infected cells. Activated T cells multiply to form an army of cells primed to combat the pathogen.

B cells, upon activation, differentiate into plasma cells that produce antibodies. Antibodies are proteins that can recognize and neutralize specific pathogens. These antibodies circulate in the bloodstream, ready to target and neutralize the actual pathogen, if encountered.

A crucial aspect of vaccination is the formation of memory cells. These cells "remember" the characteristics of the pathogen, providing long-lasting immunity. If the individual is later exposed to the real pathogen, memory cells can quickly mount a robust and targeted immune response, preventing or reducing the severity of the infection.

Challenges in Traditional Vaccine Development

Traditional vaccine production relies on large-scale cell culture, limiting rapid response capabilities during outbreaks. Efforts to develop vaccines independent of cell culture related hurdles, prompted the researchers to explore alternatives to meet the demands of emerging infectious diseases.

The Promise of mRNA Vaccines

In the early 1990s, Hungarian biochemist KatalinKarikó faced challenges in developing mRNA therapies but stayed dedicated. Despite funding difficulties, she worked persistently on her vision. Partnering with immunologist Drew Weissman, they studied how different RNA types interact with the immune system. This teamwork not only paved the way to overcome challenges but also pushed the development of mRNA technology for clinical use. Karikó and Weissman made important contributions to the scientific understanding and use of mRNA, marking a crucial step forward in this groundbreaking therapeutic approach.

The Breakthrough

Karikó and Weissman studied dendritic cells and found that *in-vitro* transcribed mRNA caused inflammatory reactions upon cell entry. Recognizing the significance of modifying nucleoside bases, especially substituting uridine with pseudouridine, they successfully made mRNA non-immunogenic. Their groundbreaking work, documented in key studies in 2005, set the stage for additional findings in 2008 and 2010. These discoveries highlighted the potential of base modifications to reduce inflammation and improve protein production.

Realization of mRNA Vaccines

As the interest in mRNA technology grew, different companies started using it. They initially looked at the Zika virus and MERS-CoV. But the big challenge came when COVID-19 hit the masses. The quick development of base-modified mRNA vaccines for SARS-CoV-2 during the pandemic showed how well the method can be adapted effectively. These vaccines, with reported protection of about 95%, got approval in December 2020. This was a huge step in the history of vaccines, showing that mRNA technology can be fast and successful in responding to urgent health threats.

Global Impact and Future Prospects

mRNA vaccines have made a global impact, with over 13 billion doses given worldwide. They didn't just save lives and stop severe sickness; they helped societies to get back to normalcy. In the future, it is envisaged that this potent mRNA technology can do much more than fighting infections; it may be capable of delivering important proteins and treating serious conditions like cancer and HIV.
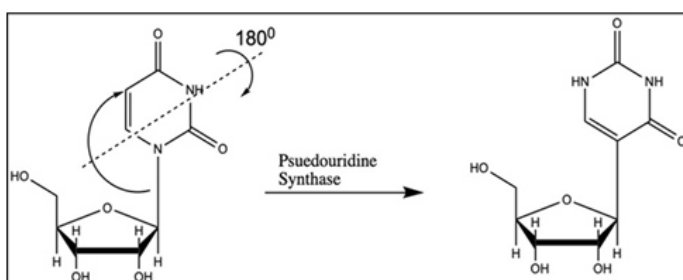
- Both are rotational isomers
- The ONLY difference is rotation of 180°
  Resulted in different bonding pattern

Fig.: Conversion of Uridine to Pseudouridine by enzyme Pseudouridine Synthase; rotation of bond by 180° changes their hydrogen-bonding ability with their partner nitrogenous bases.

BEAM
TECHNOLOGIES
in BARC

Dr. Pitamber Singh

The book elucidates different aspects of electron accelerators and their development work in BARC. Accelerators and their applications have now become an integral part of everyday life. They are deployed not only in basic research but also for reaping wider societal benefits. Electrons being fundamental particles, they are highly preferred for basic research. Electron accelerators are extensively deployed in diversified areas, including food irradiation, industry, environment, national security, synchrotron radiation sources, healthcare to mention but a few. Electron beams are being extensively used in testing of electronics systems for ascertaining potential radiation damage in the environs of outer space during outer space missions.

Beam Technology Development Group, BARC made immense contributions towards building both DC and RF electron accelerators, particularly for industrial applications. This book poignantly presents the development journey of electron linacs at BARC. It has a total of 36 chapters written mostly by subject experts. Specifically, chapter 24 of the book discusses the basic theory of electron linear accelerators and important parameters associated with them. It not only covered the details of different systems (electron gun, power supplies, vacuum systems, accelerating structures, RF and cooling systems, etc.) but also their applications in diversified fields. Chapter 36 presents a detailed account of neutron production using electron beams generated directly through (e^-, n) and indirectly using (gamma, n) reactions. It is encouraging to note that a few hundred MeV electron accelerator had been used as to demonstrate the working of Accelerator Driven System (ADS) for Thorium utilization.

In the book, a full chapter has been devoted to human and machine safety related issues. Shielding is one of the very important aspects of accelerators. Electron linacs deliver large current/power beams and therefore, special attention needs to be given to the cooling of different systems, particularly for accelerating cavities, magnets and titanium foil through which beam emanate and strike the objects to be irradiated sufficiently. For this purpose, scanning magnets are used. The resonating frequency of the accelerating RF cavity is a strong function of temperature of the cavity. The book presents details on thermal analysis of these systems.

In a nutshell, the book is a compendium of articles with information on the evolution and transformation of beam technologies development in BARC. I am confident that it will surely enlighten and excite the community of young researchers.

Dr. Pitamber Singh, an outstanding scientist, joined BARC in 1976 after graduating from the 19th batch of BARC Training School. Dr. Singh made important contributions towards indigenous development of accelerators. Besides, he also made several important contributions in the field of nuclear physics. He has more than 400 publications to his credit, which includes 84 in internationally reputed journals. Dr. Singh had been a recipient of DAE's Technical Excellence Award for the year 2000. He worked at Max Planck Institute for Kernphysik, Heidelberg, as post doc Fellow during 1985-86, and has visited several accelerator laboratories. Presently, he is the Chairman of DAE's Design and Safety Review Committee-Accelerator Projects (DSRC-AP).
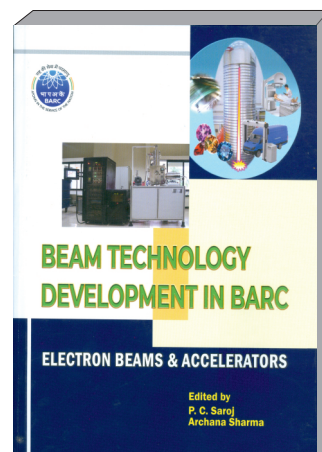
Reports from conferences, theme meetings and workshops

Participants of Training Course pose for a group photo during the valedictory function.

46ᵗʰ Training Course
on Safety and Regulatory Measures for BARC Facilities

The BSC Secretariat (BSCS) conducts short-term training courses for the personnel working at BARC facilities as part of its mandate. One such regular training course is on "Safety and Regulatory Measures for BARC Facilities". The 46ᵗʰ course in this series was conducted during October 11-14, 2023 at BARC(F) Auditorium, Atchutapuram, Visakhapatnam. Seventy-four participants from ESS(V), CES(V), CAD(V), PP&EMD, ALWRD, NCCCM (Hyderabad), REPMP, and A&MPD(V) attended the course.

During the inauguration of the training course, Rajvir Singh welcomed the Chief Guest, senior officers, invitees and participants. Clement C. Verghese, Chairman, BARC Safety Council (BSC) introduced the course and explained its relevance to the participants. The Chief Guest of the function, K. Srinivas, Director, ESG & PD, BARC(F), Visakhapatnam explained the importance of safety and emphasized on the various safety aspects considered during the construction of the facilities. He elaborated the role of BSC for ensuring safety in BARC Facilities. He also appreciated the efforts of BSCS for conducting this safety program at BARC(F). C. L. R. Yadav, Course coordinator, proposed the vote of thanks.

The training course was conducted through classroom lectures and video displays. It covered topics, such as regulatory framework of BARC; radiation basics and natural radiation; construction, industrial, accelerator and electrical safety; regulatory inspections; event reporting and improvement of safety culture in the facilities.

In addition to the faculties from BSCS, experts from AERB; NPCIL, Mumbai, Industrial Hygiene & Safety Section and faculties from BARC(F) have shared their knowledge and experiences to the participants. The valedictory function was graced by Chief Guest D. Venkateswarlu, Former PD, BARC(F), Guest of Honor M.S. Rao, Head, TL-5 Visakhapatnam, N. S. Joshi, Head, BSCS and senior officers of BARC (F). The training program was well appreciated by the participants and other dignitaries.

Reports from conferences, theme meetings and workshops

Delegates of 4-day national workshop Atomistic Modeling of Molecules and Materials (AMMM-2023).

AMMM-2023

National Workshop on
Atomistic Modeling of Molecules and Materials

A four-day national workshop 'Atomistic Modeling of Molecules and Materials' (AMMM-2023) was organized during December 11-14, 2023 at Multipurpose Hall, TSH, BARC, Mumbai under the auspices of DAE-BRNS. Chemical Engineering Group, BARC and the Society for Atomistic and Continuum Modeling (SACM) spearheaded the workshop activities. The welcome address at the workshop was made by Dr. Sulekha Mukhopadhyay, Head, Chemical Engineering Division, BARC. K.T. Shenoy, Director, Chemical Group and Chairman, AMMM-2023 made the introductory remarks. Prof. A.K. Tyagi, Director, Chemistry Group and Bio-science Group, BARC as the program chief guest delivered the workshop inaugural address. In his inaugural speech, Prof. Tyagi highlighted the need of atomistic modeling based multi-scale approach for advanced scientific research. He also stressed the importance of synergy between Atomistic Modeling aspects such as theory, computation and experimentation in different branches of sciences and engineering for proper outcomes. The proceedings copy of the workshop was released by the chief guest. The inaugural program vote of thanks was delivered by Dr. Sk. Musharaf Ali, Head, AMCAS, ChED and Convener, AMMM-2023. Close to 175 delegates from DAE and non-DAE institutes participated in the 4-day workshop. A total of 36 invited lectures and 56 flash presentations were covered in the field of atomistic modeling comprising electronic structure calculations such as density functional theory, equilibrium and non-equilibrium statistical mechanics, molecular dynamics and Monte Carlo simulations. Machine learning-driven atomistic modeling was also discussed. Experts from various institutes, including IISc, TIFR, IACS (Kolkata), JNCASR, IITs (Mumbai, Chennai, Patna, Hyderabad, Jodhpur), ICT (Bhubaneshwar), IISER (Pune), CEBS (Mumbai), IGCAR (Kalpakkam) and BARC made presentations on several aspects of atomistic modeling. Participants of the workshop were presented with certificates by the prestigious Royal Society of Chemistry.

Dr. Pooja Sahu, Scientific Officer, Chemical Engineering Group, BARC, was awarded Atomistic Modeler of the Year-2023 plaque by the Royal Society of Chemistry at the workshop.

Reports from conferences, theme meetings and workshops

33rd Annual Conference & Exhibition on
Non-Destructive Evaluation & Enabling Technologies

The 33rd Annual Conference & Exhibition on Non-Destructive Evaluation and Enabling Technologies (NDE-2023) was organized by Indian Society for Non-Destructive Testing (ISNT), at Pune during 7-9 December, 2023. The conference was inaugurated by Dr. Samir V. Kamat, Secretary, DD, R&D and Chairman, DRDO.

Dr. V. Narayanan, Director, LPSC, ISRO was the guest of honour. Dr. P. P. Nanekar, Head, PIED, BARC chaired the session on Advances in Ultrasonics. Dr. V. H. Patankar, Head, UIEFS, ED, BARC delivered an invited talk on 'Challenges in the development of Ultrasonic Imaging systems for NDT of critical components and structures'. Dr. Lakshminarayana Yenumula, SO/F, ITIS, BARC, Anant Mitra, SO/E, ITIS, BARC, Jyoti Gupta, SO/D, RMD, BARC, Jothilakshmi N., SO/F, QAD, BARC, Rakesh Kumar Pal, SO/D, QAD, BARC presented research papers in the conference.

Around 200 research papers were presented by Indian and international researchers and the conference was attended by more than 900 participants. Chief Guest of NDE-2023 conference emphasized the need to generate a roadmap for Non-Destructive Evaluation policy for the Indian Industry, for the Amrit-Kaal-India@2047.

Outreach Program in Jammu

As part of pan-India outreach on atomic energy activities in India, a team of scientists & engineers of BARC visited various colleges of Jammu during 9-13 October, 2023. The BARC team visited Central University of Jammu, University of Jammu, Maulana Azad Memorial Cluster University in Jammu, Shri Mata Vaishno Devi University in Katra and IIT- Jammu. At each of these colleges, the visiting BARC officials organized a range of student-centric activities, including quiz program on science and technology topics, lectures on a range of ongoing research and development activities in atomic energy fold, and edutainment skits on nuclear energy.

The BARC team present in Jammu during the entire 5-day program included S.K. Mondal, S.P. Prabhakar, Heema Rao, R.K.B Yadav, R.K. Mishra, Yatin Thakur, Ram Badade, Atul Likhite, Umesh Gulane, Pradeep Pawar and Samruddhi Patil. Dr. S. Adhikari, Associate Director, Knowledge Management Group, BARC, functioned as the program convener.

On the final day of the program, Dr. Archana Sharma, Director, Beam Technology Development Group, BARC, delivered a talk on Beam technology for the benefit of the participants.

The 5-day program witnessed participation of more than 1200 students.

DR. HOMI N. SETHNA BIRTH CENTENARY
Celebrating the legacy of an atomic visionary gifted with original thinking and innovation

Dr. Homi N. Sethna (1923-2010)

"…Dr. Sethna gave immense thrust to indigenous efforts for development of novel fuels, which have instilled a great sense of pride among the atomic energy community amidst a difficult period when the country was finding it tough to source fuel requirements for its expanding nuclear fleet.

Dr. Ajit Kumar Mohanty
Chairman
Atomic Energy Commission

"…A remarkable trait of Dr. Homi Bhabha was to judge the capabilities of an individual from his very first contact… Dr. Homi Sethna was one of those outstanding individuals

Dr. R. Chidambaram
Former Chairman
Atomic Energy Commission
&
Former PSA to Govt. of India

Glimpses of Birth Centenary Function (Clockwise from top): Inauguration of bust of Dr. Sethna by Chairman, AEC and Director, BARC; release of publication on the pioneering achievements of Dr. Sethna; group photo of program organizing committees.

"…A true visionary, Dr. Sethna's name figures in the list of stalwarts who showed unflinching commitment in treading the atomic energy program towards the goal of greater indigenization

Vivek Bhasin
Director
Bhabha Atomic Research Centre
&
Member
Atomic Energy Commission

"…Indian nuclear programme consolidated its self-reliance in the wake of embargos following 1974 PNE under his (Dr. Sethna's) leadership

Dr. Anil Kakodkar
Former Chairman
Atomic Energy Commission
&
Chancellor
Homi Bhabha National Institute

The birth centenary of Dr. Homi Nusserwanji Sethna served as yet another perfect occasion for the Department of Atomic Energy family to recall the memories of India's atomic energy program from the pioneering days of the 1940's. The Department of Atomic Energy and a galaxy of constituent units, including BARC and NRB have joined hands to celebrate the legacy of Dr. Homi N. Sethna, considered one of the brightest engineers of the department, who served as Director, BARC (1966-1972) and later as Chairman, AEC during 1972 to 1983. A one-day program was organized at BARC campus in Mumbai, which saw participation of DAE scientific community from past to present.

Dr. Sethna, working in tandem with nuclear energy pioneer Dr. Homi J. Bhabha, left his imprint on numerous programs of DAE by rapidly operationalizing important activities, which include the establishment of Uranium Metal Plant and Thorium Plant initially, soon followed by the establishment of maiden Reprocessing Plant (Plutonium Plant). Dr. Sethna also led the program for major expansion of heavy water production capacity in the country and offered necessary impetus for driving domestic research towards development of new heavy water technologies.

BARC
CHINTAN BAITHAK
brainstorming science & technology for cutting edge in-house R&D

@High Flux Research Reactor

Salient Features

Reactor type and Power: Open Pool Type, 40 MW (Th)

Maximum In-Core Thermal Flux: $1 \times 10^{15} n/cm^2/s$

Maximum Thermal Flux in Reflector Vessel: $5 \times 10^{14} n/cm^2/s$

Maximum Fast Flux: $2.5 \times 10^{14} n/cm^2/s$

Bhabha Atomic Research Centre (BARC) has been the front-runner in the Indian Nuclear Research Reactor Programme, having built and operated a number of research reactors of various types and capabilities. In order to further enhance the Indian Nuclear programme, High Flux Research Reactor (HFRR) is proposed to be constructed at BARC Campus, Vizag for providing advanced capabilities in the field of basic and applied research. A brief update of major design philosophy, salient features, reactor core components, process systems, main I&C systems, including safety classification, various development activities and utilisation facilities having state of art features is presented here.

Reactor Core

Fuel: LEU, Plate type geometry

Moderator and Coolant: Light Water

Reflector: Heavy Water in annular reflector vessel

Control Devices: Hafnium Absorber assemblies, Heavy water reflector dumping

Major Reactor Utilization

- Beam Tube Research including Cold Neutron Source

- Fuel irradiation studies

- Material irradiation studies

- Radiochemistry programmes including neutron activation analysis

- Fission Moly production

- Production of NTD silicon

- Isotope production

Speakers
1. Joe Mohan 2. Monesh Chaturvedi
3. Aniruddha Ghosh 4. Istiyak Khan

Key resource persons
Joe Mohan, Associate Director, RPG
Dr. Samiran Sengupta, Head, RRDPD

Contributors
Reactor Projects Group, Reactor Design & Development Group, Reactor Group, Nuclear Fuels Group, Materials Group, Electronics & Instrumentation Group, Engineering Services Group, Physics Group, Health Safety & Environment Group, Nuclear Recycle Group, Multi-disciplinary Research Group, Chemical Engineering Group & BARC Safety Council.
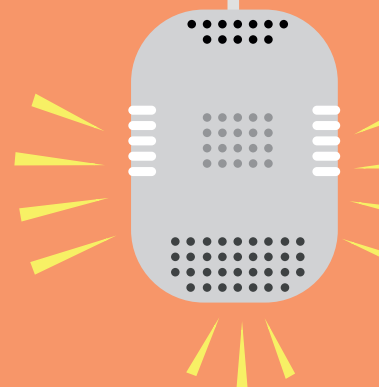
trombay colloquium*
October 5, 2023

Studying Galaxy Evolution
with the GMRT

Galaxies are not static, but evolve with time. One important process that takes place as galaxies evolve is the conversion of gas into stars. On a cosmic scale, it is well established that this star formation activity peaked about 10 billion years ago and that the average star formation rate of the universe has declined sharply since then. Atomic Hydrogen is the primary fuel for star formation, stars form as the gas cools to become molecular hydrogen, and then cools further and collapses under self gravity. Understanding the evolution of the atomic hydrogen content of galaxies is hence key to understand the evolution of the star formation rate with cosmic time. Unfortunately, because of the difficulties in detecting atomic hydrogen emission (via its best tracer, the 21 cm spectral line), until recently very little was known about the evolution of the gas content of star forming galaxies. I will discuss results from ongoing atomic hydrogen surveys of star forming galaxies using the upgraded Giant Metrewave Radio Telescope that have significantly added to our understanding of the evolution gas in galaxies.

Prof. Jayaram N. Chengalur
Director
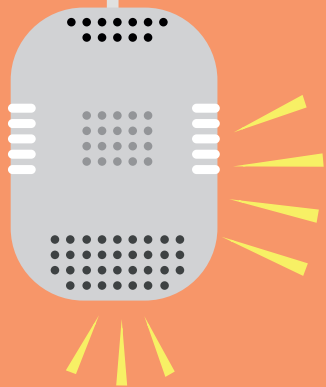**Tata Institute of Fundamental Research**

*The Trombay Colloquium is a key window of opportunity for the BARC community to brainstorm with eminent individuals belonging to a wide spectrum of science and allied domains. Prominent scientists and technologists are invited to BARC Trombay to deliver captivating talks on emerging domains of science, and the transformative effect of new technological innovations.

trombay
colloquium*
November 23, 2023

Economy, Energy, Ecology & AI
Some Thoughts

Relatively inexpensive fossil energy is responsible for rapid progress of humanity post industrial revolution. Energy is essential for economic growth. Capitalistic economics with advancement of diverse technologies has helped improve standard of living of increasing human population, and now digital/ AI technologies are accelerating this progress. With technological progress there's consolidation of power, wealth inequality, ecological distress, biodiversity loss, etc. Human activities have perhaps altered the Earth beyond repair for humanity to continue to prosper forever. There is an optimistic view that green energy, electrification and decarbonization may mitigate impending ecological disasters. Is this triumph of hope versus practical reality? Activities that give benefits in 30, 50 years has little economic motivation, as capitalism promises everything now, amplified by on demand throw away society. Are there any alternate economic and societal paradigms?

Dr. Ajit Sapre
Group President (R&D)
Reliance Industries Ltd

*The Trombay Colloquium is a key window of opportunity for the BARC community to brainstorm with eminent individuals belonging to a wide spectrum of science and allied domains. Prominent scientists and technologists are invited to BARC Trombay to deliver captivating talks on emerging domains of science, and the transformative effect of new technological innovations.

Class 10000 facility in CTS, TPD in BARC.